the Energy to Lead

FINAL REPORT

GTI PROJECT NUMBER 20582

Nonmetallic Joint Quality Assessment

DOT Prj# 217
Contract Number: DTPH56-07-T-000001

Reporting Period:
Final Report
August 1, 2007 through July 31, 2009

Report Issued (Period Ending):
July 31, 2009

Prepared For:
Mr. James Merritt
PHMSA Project COTR

GTI Contact:
Gas Technology Institute
Dr. Kiran Kothari
Institute Engineer/Program Manager
kiran.kothari@gastechnology.org
847-768-0893

Project Technical Team:
Dr. James E. Huebler
Maurice Givens
Christopher J. Ziolkowski

Gas Technology Institute
1700 S. Mount Prospect Rd.
Des Plaines, Illinois 60018
www.gastechnology.org

Legal Notice

This information was prepared by Gas Technology Institute ("GTI") for DOT/PHMSA (Contract Number: DTPH56-07-T-000001.

Neither GTI, the members of GTI, the Sponsor(s), nor any person acting on behalf of any of them:

a. Makes any warranty or representation, express or implied with respect to the accuracy, completeness, or usefulness of the information contained in this report, or that the use of any information, apparatus, method, or process disclosed in this report may not infringe privately-owned rights. Inasmuch as this project is experimental in nature, the technical information, results, or conclusions cannot be predicted. Conclusions and analysis of results by GTI represent GTI's opinion based on inferences from measurements and empirical relationships, which inferences and assumptions are not infallible, and with respect to which competent specialists may differ.

b. Assumes any liability with respect to the use of, or for any and all damages resulting from the use of, any information, apparatus, method, or process disclosed in this report; any other use of, or reliance on, this report by any third party is at the third party's sole risk.

c. The results within this report relate only to the items tested.

Table of Contents

Legal Notice ii
Table of Contents iii
Table of Figures iv
List of Tables v
Abstract 1
Executive Summary 2
Introduction 3
Background and Need 3
GTI Approach to Ultrasonic Inspection 3
Instrumentation 5
Results 7
Non-EF Socket Fusion Couplings and Tees 7
Scan pattern for non-EF couplings and tees 7
Heat affected zone in non-EF socket fusion joints 8
Detection of flaws in non-EF socket fusion joints 12
Measurement of ovality and angle of pipe insertion 18
Non-EF Saddle Tees 19
Scan patterns for non-EF saddle tees 19
Detection of flaws in non-EF saddle fusion tees 23
Detection of flaws in non-EF saddle fusion tees 26
EF Socket Fusion Couplings and Tees 28
Scan pattern for EF couplings and tees 28
Detection of flaws in EF couplings 29
EF Socket Fusion Couplings and Tees 33
Scan pattern for EF saddle tees 33
Detection of flaws in EF saddle tees 35
Results of the Automated Algorithms 38
Conclusions 43
Recommendations 43
List of Acronyms 43
References 44

Table of Figures

Page

Figure 1: A two-sensor assembly permits collection of pulse/echo (left diagram) and pitch/catch waveforms (right diagram) 4
Figure 2. Photograph of the sensor/stand-off used to collect data from non-EF socket fittings ... 6
Figure 3. A-scan waveform illustrating the need for a stand-off 6
Figure 4. Photograph of non-EF socket fusion coupling and tee 7
Figure 5: Recommended scan pattern for socket fusion coupling 7
Figure 6. The pipe and fitting are heated simultaneously by the same heating iron 10
Figure 7. The heating tool forces a taper on the end of the pipe 10
Figure 8. The heating iron alters the shape of the pipe and fitting 11
Figure 9. Material is displaced into the fitting, building up at the end of the pipe 11
Figure 10. Material is also forced around the face of the fitting 11
Figure 11. Cross-section of a joint showing displacement of fine dirt from the fusion interface. 12
Figure 12: D-scan showing diagnostic areas of a non-EF fusion joint 13
Figure 13: Photograph of excess bead inside socket tee 13
Figure 14: D-scan of socket fusion coupling with excess bead 14
Figure 15: D-scan of non-EF coupling where the pipe was short stabbed 14
Figure 16: D-scan showing a 0.092 hole in the coupling 15
Figure 17: D-scans showing V-groove in the coupling 15
Figure 18: Photograph of tee showing location of leak 16
Figure 19: D-scan showing a leak in a socket fusion tee 16
Figure 20: Photograph of pipe inserted at an angle into a tee 17
Figure 21: This D-scan shows incomplete fusion 17
Figure 22: Circumferential scan showing the pipe is at an angle or is oval 18
Figure 23: Schematic of a joint made with a pipe inserted at an angle and an oval pipe 19
Figure 24: This rectangular base permits access for inspecting the fusion area 20
Figure 25: The curved base creates challenges for inspection of the fusion area 20
Figure 26: The service tee restricts the height of the scanning mechanism 20
Figure 27: Tees with sufficiently narrow bases can have the fusion area (red line) inspected .. 21
Figure 28: Tees with a broad base require additional sensors to inspect the joint 22
Figure 29: A complex wedge is required for tee geometries in Figure 28 22
Figure 30: The pipe and saddle tee are heated simultaneously 23

Figure 31: The iron creates a rippled surface on the pipe and tee 24
Figure 32: Completion of a non-EF saddle fusion joint with excessive bead roll back..... 24
Figure 33: Same saddle fusion joint with material removed 25
Figure 34: Photograph of mechanism to collect data on the non-EF saddle tees..... 25
Figure 35: Pulse/echo D-scan for properly made non- EF saddle tee 26
Figure 36. Pulse/echo D-scan for non- EF saddle tee with two 1/8-inch holes..... 26
Figure 37. Pitch/catch D-scan for a properly made non- EF saddle tee 27
Figure 38. Schematic of selected paths in non-EF saddle tee..... 27
Figure 39. Photograph of EF socket fusion coupling with sensor and stand-off 28
Figure 40: Scan pattern for EF coupling inspection 28
Figure 41. D-scan of 4-inch EF coupling made with the proper procedures..... 30
Figure 42. Photograph of normal distortion of the inner pipe wall caused by thermal effects.... 30
Figure 43. D-scan of 4-inch EF coupling for aluminum sheet located from position 25 to 57 31
Figure 44. D-scan of 4-inch EF coupling with small aluminum disks 4.7, 2.0, and 2.4 mm 31
Figure 45. D-scan of 4-inch EF coupling with dry dirt 32
Figure 46. D-scan of 4-inch EF coupling with mud 32
Figure 47: Photograph of an EF saddle tee on a 4-inch diameter pipe. 33
Figure 48: Single sensor arrangement for EF coupling inspection 34
Figure 49: Scan pattern for EF saddle tee inspection..... 34
Figure 50: Sensor on stand-off for EF saddle tee inspection..... 35
Figure 51: D-scan for a correctly made EF saddle tee 36
Figure 52: D-scan for an EF saddle tee with thin plastic insert and oily glove wipe..... 36
Figure 53: Photograph of failed 2-inch EF saddle joint 37
Figure 54: D-scan of EF saddle tee made similar to ones that failed 37

List of Tables

Table 1. Predictions and results for yellow 2-inch diameter non-EF couplings..... 40
Table 2. Predictions and results for orange 2-inch diameter non-EF tees..... 41
Table 3. Predictions and results for yellow 4-inch diameter non-EF saddle tee fittings..... 41
Table 4. Predictions and results for yellow 4-inch diameter EF couplings..... 42

Abstract

The objective of this project is to develop nondestructive evaluation (NDE) methods for inspecting all non-metallic heat fusion joints, including electro-fusion (EF) joints. The natural gas industry has a large investment in developing and installing polyethylene (PE) pipe. Today, PE is the predominant pipe used in gas distribution systems. The industry developed techniques for joining pipe and fittings with visual inspection verifying joint quality. Visual inspection of PE joints works in most cases, but does not guarantee integrity. Field failures demonstrate the need for more rigorous inspection techniques. There is currently no easy to use tool for non-destructively inspecting PE joints. An ideal inspection technique must require no ultrasonic expertise on the part of the operator, be expandable to new pipe materials and sizes at low cost, and be implemented in low cost hardware.

This DOT/PHSMA project expands and adapts a technique originally developed for inspection of butt fusion joint joints to inspection of both socket fusion joints and electro-fusion joints. The ultrasonic non-destructive evaluation (NDE) technique does not require the operator to view or interpret ultrasonic data. The inspection technique models the geometry and physical properties of the joint to obtain the independent variables. The dependent variables are determined by ultrasonic measurements on a small number of good quality joints. Once the dependent variables are captured, it is not necessary to make measurements on bad joints. This ultrasonic inspection technology provides the following advantages over what is currently available:

- Provides an unambiguous joint pass-fail indication to the operator
- Simple adaptation to new pipe materials and sizes
- Algorithm can run on inexpensive electronics
- Can measure pipe ovality and insertion angle on completed joints
- Can detect excess bead on internal surfaces of joints.

Executive Summary

The objective of this project is to develop nondestructive evaluation (NDE) techniques for inspecting all types of non-metallic fusion joints, including electro-fusion (EF) joints. Visual inspection of PE joints works in most cases, but does not guarantee joint integrity. Field failures demonstrate the need for more rigorous inspection techniques. There is currently no easy to use tool for non-destructively inspecting PE joints. Previously, an ultrasonic testing standard, ASTM D 1598, was developed to inspect butt fusion joints. It was withdrawn because the differences in operator skill made the results too variable. Subsequently, Gas Technology Institute (GTI) sponsored development of a commercial ultrasonic product, UltraMc®, for butt fusion joints. The unit was a technical success and some units are still in use. However, the unit also required a skilled operator and was considered too expensive. This led to insufficient sales and the product was discontinued in 1999. Other research organizations are currently developing ultrasonic phased array inspection tools. Although the resulting visual displays of fusion joints are spectacular, they require expert interpretation and hardware costing thousands of dollars.

GTI, under the sponsorship of Operations Technology Development, NFP, is developing an ultrasonic NDE technique for discriminating good from bad PE butt fusion joints. It does not require the operator to view or interpret ultrasonic data. The technique models the geometry and physical properties of the joint to obtain the independent variables. The dependent variables are determined by ultrasonic measurements on a small number of good quality joints; it is not necessary to make measurements on bad joints. This combination makes the cost of adapting the technique to a new pipe material or pipe size low. In the initial testing, the technique correctly assessed 53 out of 53 butt fusion joint conditions. A low hardware-cost ultrasonic inspection unit is possible based on this technology.

This DOT/PHSMA project expands that approach to develop inspection techniques for both heat fusion joints and electro-fusion joints. The approach was successful on yellow PE2406, 2-inch diameter non-EF socket fusion couplings; where an automated algorithm correctly assessed 31 out of 34 fusion areas. The same algorithm was applied to orange PE2406 2-inch diameter tees that had failed in the field, correctly identifying those fusion joints as bad. An automated algorithm also correctly classified 8 out of 8 D-scans in 4-inch diameter non-EF saddle tees. Results for yellow PE2406, 4-inch diameter EF couplings were mixed, including missing a flaw that is detectable with a visual inspection of the waveforms. Late in the project, it was discovered a simple adjustment that can be made to the data that will improve the quality of EF coupling joint assessment. This discovery came too late in the project to be tested. Scan patterns for collecting the data were developed for each of these fittings. Hardware can be developed to implement these scan patterns.

Flaws in non-EF and EF saddle tees were detected. However, the huge variety of saddle tee geometries makes it difficult to develop a single scan pattern to assess quality. In addition, the body of the tee prevents collecting data for the entire fusion surface. It is not known if inspecting less than 50% of the fusion surface will result in reliable assessment of the entire saddle tee joint.

During this project, GTI discovered it is possible to use the ultrasonic measurements to determine the pipe ovality and the angle of pipe insertion into the fitting after the joint is complete. The initial quality of the fusion interface can be acceptable; however joints are known to fail with time if ovality or insertion angle is excessive. There is an ovality standard. An insertion angle standard would need to be developed in the future.

The ultrasonic technique can also detect excess bead on interior surfaces of various joint types. It is known that when socket fusion couplings and tees are made, plastic melt material can be displaced to form stress risers inside the joint. In the future, it would be needed to determine the relationship between the distribution of the displaced material and eventual failure of the joint.

Introduction

Background and Need

The gas distribution industry has been successfully using plastic pipe for decades. Plastic pipe, couplings, tees, and saddle tees are joined with heat and EF fusion. Electrofusion (EF) couplings and saddle tees have a coil of wire imbedded in the fitting. The pipe surface is scraped to remove the outer layer before being inserted into the coupling. An electric current passes through the coil, melting the surface layers of the fitting and pipe. Thermal expansion forces the material together forming a joint which remains after the cooling. A non-EF socket fusion fitting (coupling or tee) and pipe are cleaned and then heated simultaneously with an external iron. The heating iron is removed and the parts pressed together. In butt fusion, the pipe ends are faced, heated with an external iron, and pressed together. The industry has developed detailed fusion procedures, which if carefully implemented by well-trained operators will yield joints that are as strong as or stronger than the native pipe material.

The commonly used inspection technique is visual observation. In the case of butt fusion, the size and shape of the rollback bead is observed during melting and after the fusion process. The quality of the fusion process is harder to observe in EF and non-EF fittings. Visual inspection is subjective and dependent on operator skill and experience. A simple, reliable and cost-effective technique and instrument that quantitatively assesses heat fusion joint quality is needed. The benefits of an inspection tool include: 1) Higher reliability than visual inspection, 2) Determination of joint quality while the operator is still present and can replace the joint, and 3) The ability to retroactively inspect suspect joints that have been in service many years without removing the joint from the pipeline.

Ultrasonic inspection is seen as the answer to the fusion joint quality inspection problem. Many attempts (refs 1-18) have been made to utilize ultrasonic inspection for plastic joints, with most of this work for butt fusion joints. ASTM F600-78 “Standard Practice for Nondestructive Ultrasonic Evaluation of Socket and Butt Joints of Thermoplastic Piping” (ref 2) was issued for the manual ultrasonic inspection of butt fusion welds in polyethylene pipe. It was withdrawn in 1991 because the results were so heavily dependent upon the skill of the operator. GTI sponsored research with the goal of minimizing the ultrasonic expertise required. Two inspection instruments were developed (refs 3-11). The most successful was the UltraMc® with approximately 70 units being sold, a few of which are still being used. The general consensus was that the UltraMc was effective, but required too much ultrasonic expertise on the part of the operator and was too expensive. Another disadvantage to the instrument was its use of a neural network for classification. A neural network requires training on every flaw type that one wishes to discriminate against. This is a lengthy and costly procedure that must be repeated for each pipe material, diameter, and wall thickness.

Many developments in ultrasonic technology and signal processing have occurred in recent years, enabling improved ultrasonic inspection. One approach under development is to use ultrasonic phased arrays (refs 12-14). A phased array is composed of many piezoelectric elements stacked together. Each element is independently controlled to form an image. Although the images produced with phased arrays are impressive, the equipment is expensive and requires a well trained operator to interpret the results. As a consequence, phased array inspection may not be acceptable for day to day use.

GTI Approach to Ultrasonic Inspection

Operations Technology Development (OTD) sponsored GTI to develop a different approach that would reliably assess butt fusion joints with minimal ultrasonic expertise by the operator and could be implemented with inexpensive hardware (ref 18). That project provided cofounding for this PHMSA project.

The butt fusion inspection technique uses two sensors, each mounted on a PE wedge. As illustrated in Figure 1, the sensor assembly is centered over the fusion plane. Data is collected in both the

pulse/echo mode (ultrasound reflected from the joint) and in the pitch/catch mode (ultrasound passing through the joint). GTI developed a parametric model to assess fusion quality that uses the joint geometry, acoustic properties of the plastic material, wave propagation, and shape and amplitudes of both pitch/catch and pulse/echo paths. GTI experimentally found high quality fusions result in nearly identical ultrasonic waveforms; while poor quality fusions are noticeably and detectably different. The model requires a modest number of independent parameters to assess joint quality. In addition, it proved possible to acquire waveforms from a small number of good joints and use selected values from those waveforms as the dependent parameters. It is not necessary to test flawed joints, as is required by neural network approaches. A good quality joint passes all of the parameters. A bad joint fails one or more parameters. The technique does not require the operator to view, let alone, interpret ultrasonic data. The pair of sensors is placed on the pipe and the condition of that portion of the joint is determined. The remainder of the joint is inspected by circumferentially moving the pair around the pipe, or alternatively, a stationary array of sensor pairs can be placed around the joint like a collar. The small number of parameters in the parametric model combined with the modest testing required to obtain the dependent parameters, means the model can be inexpensively applied to all plastic pipe materials and pipe diameters.

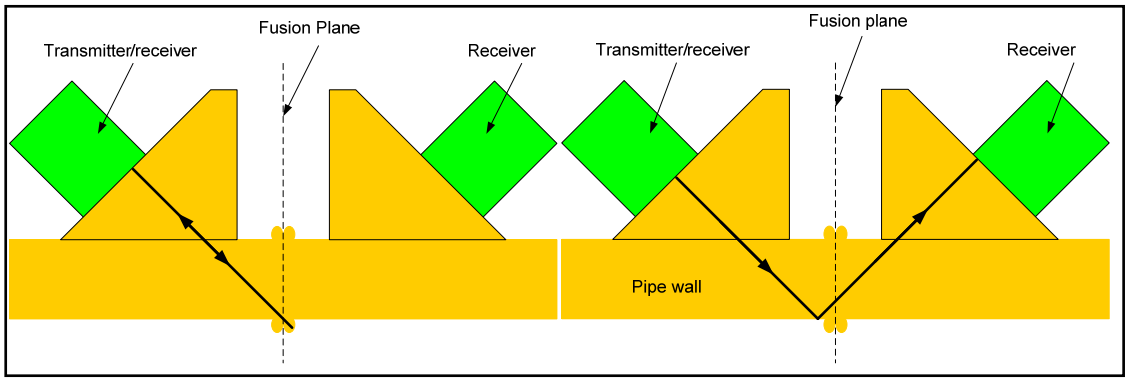

Figure 1: A two-sensor assembly permits collection of pulse/echo (left diagram) and pitch/catch waveforms (right diagram)

There are four important advantages to the technique:

- Discrimination decisions can be made automatically without the operator viewing the waveform. This minimizes the expertise and experience needed by the operator, which was a major disadvantage of previous ultrasonic testing techniques. It is a major advantage over phased array ultrasonic equipment which requires a well trained operator.

- The independent parameters are few in number and can be determined from the geometry and physical properties of the joint. This facilitates portability across materials and pipe geometries.

- The number of joints required to determine the dependent parameters is small. Only good joints need to be tested.

- The potential exists for a very inexpensive, joint inspection system.

The technical approach to this PHMSA project was to adapt the technology developed in the OTD project and develop scan patterns and data analysis techniques to inspect non-EF socket fusion couplings, non-EF socket fusion tees, non-EF saddle fusion tees, EF couplings, and EF tees.

Instrumentation

The project progressed in an iterative manner with techniques and results from one type of fitting used to make improvements in the others. After testing a variety of sensors, GTI selected an Olympus/Panametrics C543 ¼-inch diameter 5.0 MHz sensor to collect all of the data. The sensor was driven by a Panametrics 5077PR Square wave Pulser/Receiver. A ¼ diameter sensor was chosen over ½ and 1-inch sensors because of its higher spatial resolution along the scanning axis. Panametrics C series of sensors are designed for time-of-flight diffraction measurements. They are highly damped longitudinal wave transducers to provide excellent time resolution. Selecting 5.0 MHz sensors also helps with the time resolution. Medium and high-density PE pipe is highly attenuating to ultrasonic waves. All measurements were made on 2 and 4-inch fittings and it proved possible to observe the flaws with a 5 MHz sensor. For larger fittings and pipe, the larger travel distances will have more attenuation and may require lower frequency sensors because attenuation decreases with frequency. Measurements were made using longitudinal waves. Shear waves require a stiffer couplant, thus the use of longitudinal waves simplifies automated application of the technique. It is recognized the shear waves can provide additional information on the quality of the joint.

The sensor was mounted on a stand-off custom designed for the fitting being tested. Figure 2 shows a stand-off with the base machined to match the curvature of the fitting. The stand-off has two important functions as illustrated by the A-scan in Figure 3: function#1 minimizing effects of the initial pulse and function #2 making measurements in the far field. The waveform features highlighted in Figure 3 are the initial voltage pulse, the first and second reflections from the stand-off/fitting interface, and the reflection from the interior pipe wall. In order to create the ultrasonic pulse, a large voltage is applied to the piezoelectric element in the transducer. Because the transducer also acts as the detector, the initial pulse masks any reflections until there is time for the waveform to decay sufficiently. The stand-off minimizes effects of the initial voltage spike by increasing the time before a signal arrives from the material under test. The stand-off also ensures all of the material is inspected in the far field. Because sensors have a finite diameter, interference patterns are formed close to the sensor face in what is called the near-field. As a consequence of the interference patterns, the near-field sensitivity of the transducer oscillates as a function of distance from the face. In the far field, the oscillations stop and the sensitivity monotonically decays with distance. In addition, the height of the stand-off needs to be selected so the second reflection from the stand-off/fitting interface arrives after the first reflection from the inner wall of the pipe. This avoids possible confusion if the couplant between the stand-off and fitting is not optimum. The stand-off is made from the same material as the pipe to minimize reflection from the stand-off/fitting interface.

Figure 2. Photograph of the sensor/stand-off used to collect data from non-EF socket fittings

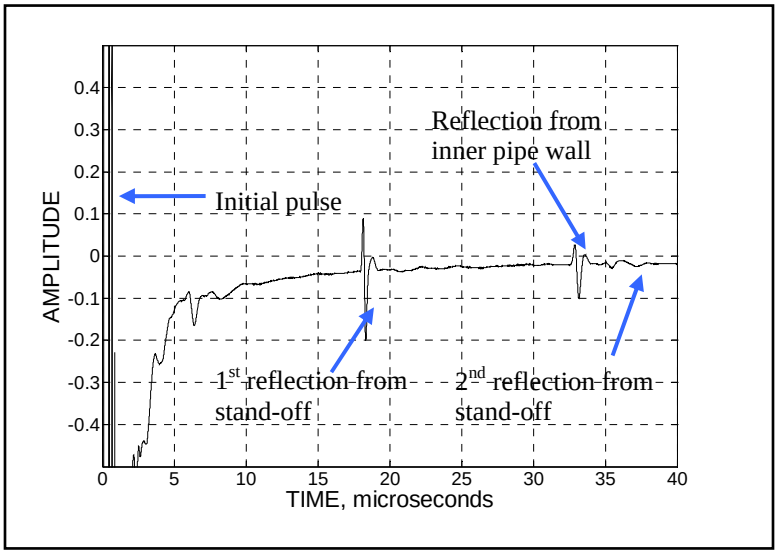

Figure 3. A-scan waveform illustrating the need for a stand-off

Results

Non-EF Socket Fusion Couplings and Tees

Scan pattern for non-EF couplings and tees

Figure 4 is a photograph of a 2-inch diameter non-EF socket fusion coupling next to a socket fusion tee. Figure 5 is a schematic of the recommended scan pattern for both. The socket coupling fusions were made with 2-inch yellow pipe MDPE Driscoplex™ 6500 PE2406 SDR 11. The couplings are Central Plastics PE2406. Measurements were also made on two 2-inch tees made from orange MDPE PE2306 SDR 11 of unknown manufacture. The tees are field failures donated by a utility to GTI.

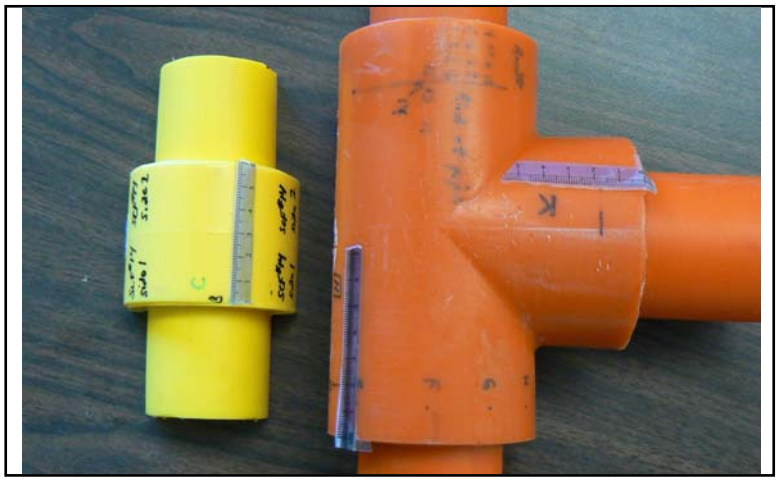

Figure 4. Photograph of non-EF socket fusion coupling and tee

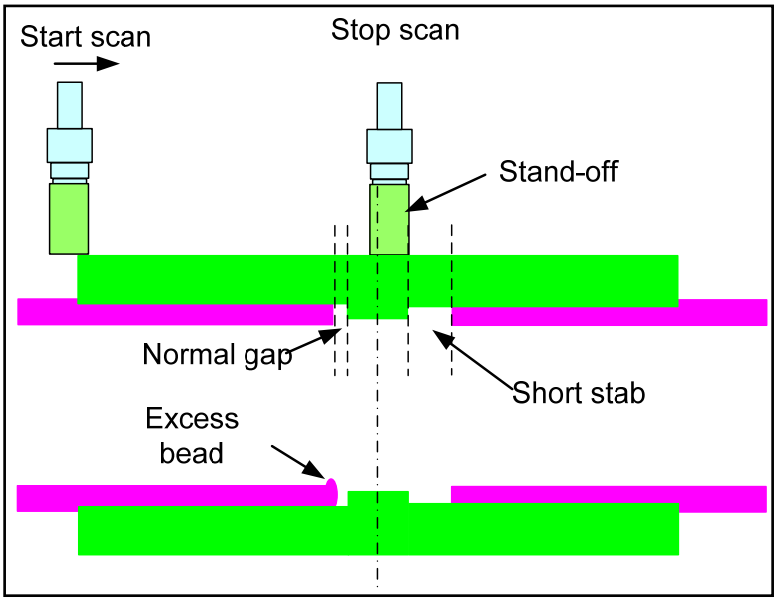

Figure 5: Recommended scan pattern for socket fusion coupling

GTI recommends that data collection for socket fusion couplings and tees use a single sensor mounted on a stand-off. The mechanical device should be designed to scan ½ of the coupling. The sensor is oriented perpendicular to the fitting and data is collected in pulse/echo mode. As illustrated in Figure 5, the scan motion is to be parallel to axis of pipe, starting with the sensor not completely over the front edge of the fitting. The sensor is moved collecting data at each step, until the center of the fitting is reached. GTI elected to use 1 mm steps, which is one eighth of the diameter of the sensor. After a scan parallel to the pipe axis is completed, the sensor is returned to the starting position. Next the sensor position is incremented 4 mm around the circumference and another scan parallel to the pipe axis is performed. The process of scanning axially and incrementing circumferentially continues until the entire fusion interface is surveyed. To inspect the second half of the coupling, the mechanism is removed and placed on the opposite side. The advantage of this approach is the mechanism can also be used to inspect each leg of a socket fusion tee of the same diameter. Therefore, only a single mechanism is required for each diameter of non-EF couplings and tees.

A single sensor proved to be a better choice than the pair of sensors on wedges used for butt fusion inspection. If two wedges are aligned along the circumference, the curved surface of the fusion joint causes information from different portions of the joint to arrive simultaneously, making interpretation of the results difficult and obscuring smaller flaws. If the wedges are oriented parallel to the axis of the pipe, not all of the fusion interface can be inspected.

A series of axial scans was selected over a series of circumferential scans because an axial scan makes it easier to determine the length of pipe inserted into the fitting. This in turn facilitates identification of critical flaws including if the pipe has been inserted too far or not far enough. With the location of the end of the pipe established, other features can be determined.

As discussed later, the ovality of the coupling/pipe and the angle of insertion of the pipe into the fitting can be measured after the joint is made. That determination requires data from two circumferences around each end of the fitting. This data can be obtained from the axial scan data at the appropriate positions. Alternatively, two scans can be made by moving the sensor in steps around the circumference of the fitting.

The data collected on the non-EF fittings was obtained by hand-holding the sensor. The stand-offs used were 10 mm thick by 23 to 26 mm wide, with the longer dimension machined to match the curvature of the fitting. This provided stability (less rocking) during the data collection. Because a mechanism will provide better stability than hand holding, GTI recommends reducing the longer dimension to 10 mm for the inspection tool. The smaller base makes it easier to have the stand-off face conform to the surface of the fitting. This is required because the surface of the fitting is not a perfect cylinder; rather each fitting has several shallow hills and valleys that are difficult to see visually. A longer base will span several peaks and valleys. Although the couplant fills the valleys, the couplant filled gaps still cause small inconsistencies in the waveform.

Heat affected zone in non-EF socket fusion joints

Part of the inspection process is to assess the quality of the fusion interface. When fittings and pipes are manufactured, the hot PE cools at a specific rate. During the fusion process portions of the pipe and fitting are reheated enough so parts can be joined. The portion of the pipe and fittings affected by the reheating is called the heat affected zone (HAZ). Because the combined fitting/pipe is thicker than for either individual part, the cooling rate is slower than during the original manufacturing. It is known that differences in cooling rate affect the velocity of sound and the density of the PE. Ultrasonic waves reflect from changes in acoustic impedance, which is the product of density and velocity of sound. Thus the size and material property changes of the HAZ could be a diagnostic of fusion quality.

Contrary to initial expectations, measurements did not detect a HAZ in non-EF couplings. The reason for not detecting the HAZ was determined by looking more closely at the details of making socket fusion joints. Socket fusion couplings and tees are made by first placing a metal clamp (chill ring) on the pipe. The metal ring defines the length of the pipe that is heated. Next, the pipe and fitting are heated simultaneously by the same heating iron as shown in Figure 6. Figure 7 shows the end of the hot pipe just after the heating iron was removed. A lip is formed at the end of the pipe as the tool is withdrawn. A socket fitting and pipe cannot be preassembled because the outside diameter of the pipe is 2.37 inch and the inside diameter of the coupling is 2.33 inch. Thus, in addition to melting the surfaces to be fused, the heating iron tapers the end of the pipe and flares the inside of the fitting. Figure 8 is a schematic of the dimensions as determined by the geometry of heating iron. As the two parts are pressed together, material must be displaced. Because they are in direct contact with the iron, it is the hottest portions that are displaced. Some of the material is pushed into the fitting and builds up at the end of the pipe as shown in Figure 9. Other portions are pushed out of the joint and are forced between the cold ring and the end surface of the fitting. A properly made joint has a characteristic flat bead at the end of the fitting as shown in Figure 10.

Figure 11 shows a cross-section of a joint where fine, dry dirt was sprinkled on the hot pipe just before completion of the joint. When this joint was ultrasonically tested, GTI did not detect a poor quality joint caused by the dirt. The reason is evident in Figure 11 because of the dirt build up near the face of the coupling. These observations are consistent if the outermost portion of the pipe, including the dirt, is scraped off toward the front face. The next layer is squeezed to the end of the pipe. Displacement of the hottest portions of the pipe and fitting from the fusion interface reduces the range of acoustic properties and explains why GTI did not observe the HAZ in socket fusions.

A second experiment was performed to confirm that the HAZ is not being detected. A piece of large-diameter PE 2406 pipe was machined to match the outside diameter of the 2-inch fitting and the inner diameter of the pipe. This simulates a joint without the fusion interface and HAZ. A-scans were collected from the machined piece of PE, from a joint made with the heater temperature (500 ^{o}F) and heating time (23 seconds) recommended by the manufacturer, and joints with heater temperatures ranging from 378 ^{o}F to 610 ^{o}F and heating times ranging from 19 to 30 seconds. There are no obvious differences among A-scans and the PE piece with no HAZ.

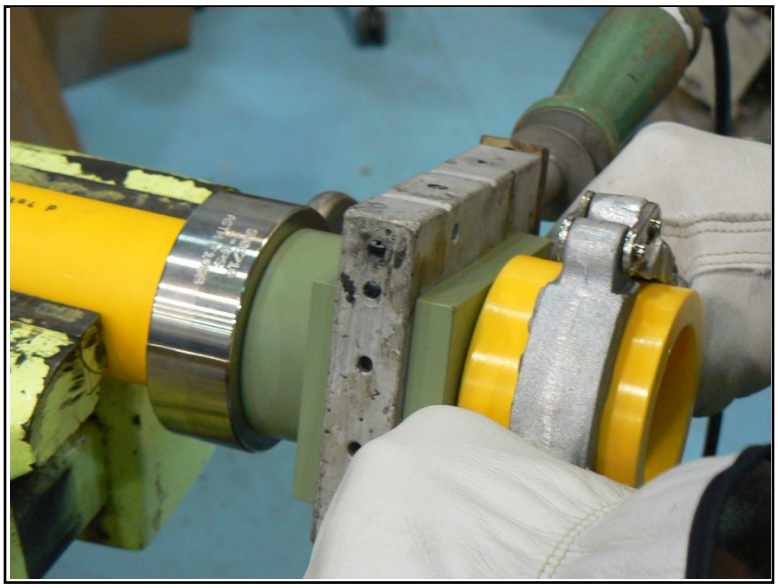

Figure 6. The pipe and fitting are heated simultaneously by the same heating iron

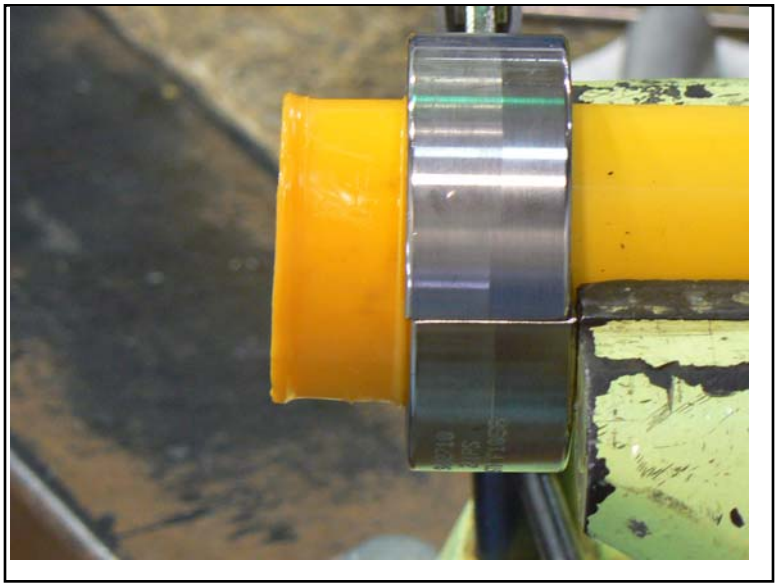

Figure 7. The heating tool forces a taper on the end of the pipe

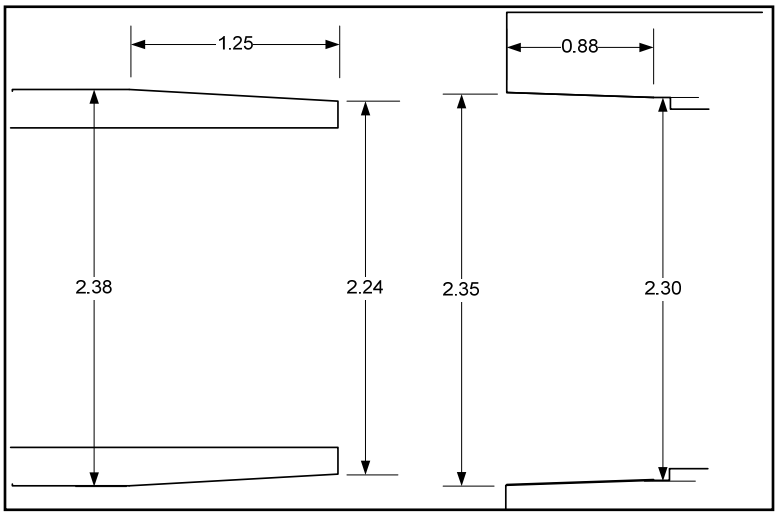

Figure 8. The heating iron alters the shape of the pipe and fitting

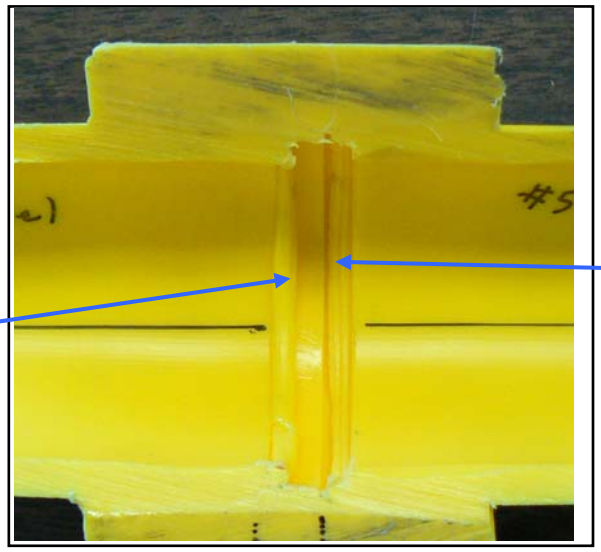

Figure 9. Material is displaced into the fitting, building up at the end of the pipe

Figure 10. Material is also forced around the face of the fitting

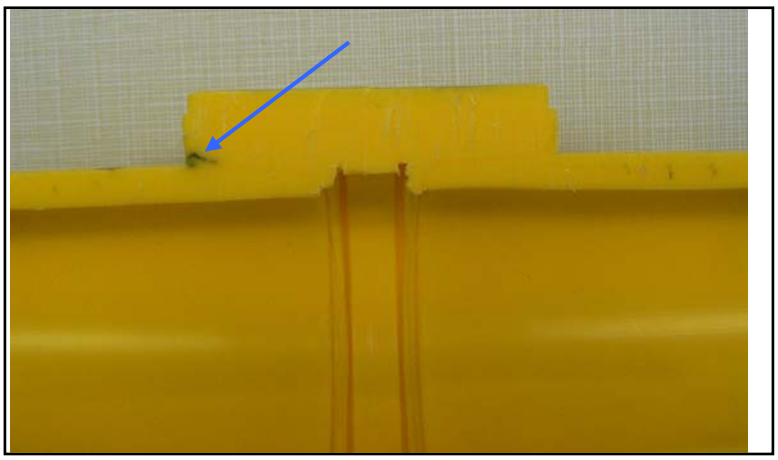

Figure 11. Cross-section of a joint showing displacement of fine dirt from the fusion interface

Detection of flaws in non-EF socket fusion joints

Figure 12 is a D-scan made parallel to the axis of the pipe/fitting. The D-scan is composed of 37 A-scans spaced 1.0 mm and is shown to illustrate concepts of the automated analysis. The x-axis of the D-scan is the position along the scan. The y-axis is proportional to the round trip time of the ultrasonic wave. The waveform is divided into 10,000 divisions, with each division being 4.0 nanoseconds. Thus, 10,000 is 40.0 microseconds. The portions of the wave form between 0 and 4800 are not shown because they are in the stand-off and, therefore, provide no information about the joint. The field-operator will not view the D-scans; the analysis of fusion quality is made by the software. A brief description of the joint geometry is needed to understand the D-scan. Figure 5 is a schematic cross-section of the pipe and one leg of the socket fitting. There is an internal step in the coupling; however, the step is not used to stop the insertion of the pipe. When properly attached, the cold ring stops insertion of the pipe short of the step. During the insertion process, some material squeezes out, building up at the end of the pipe. In a properly fused joint, there is a small gap between the step and the displaced plastic at the end of the pipe that can be observed ultrasonically.

The operator would attach the scanning mechanism to the fitting and press a start button to activate the data collection. The length the pipe inserted into the coupling is obtained by measuring the length of the reflections from the inner wall of the pipe. The first step is to determine the position of the front edge of the coupling. When the sensor is hanging over the edge of the coupling, ultrasonic waves reflect from the bottom of the stand-off attached to the sensor. As the scanning begins, the front edge of the coupling is defined when those reflections disappear and reflections from the interior pipe wall start appearing. The two traces overlap because of the finite size of the sensor. The white box on the left-hand side of Figure 12 shows the portion of the D-scan where the start of the fitting is determined. If the pipe/coupling fusion interface is defective, signals from the interior wall will not be present or will be reduced in size. Such a flaw would be flagged by another part of the data analysis. Similarly the end of the pipe (yellow box) and the internal step (violet box) inside the coupling are detected. The step between the end of the pipe and the internal step is detected in the green box. Reflections from the inner pipe wall are detected in the horizontal white box. Lack of fusion is detected in the horizontal yellow box. The software measures the amplitudes in each of these boxes and compares them to the small range of values that define a good joint.

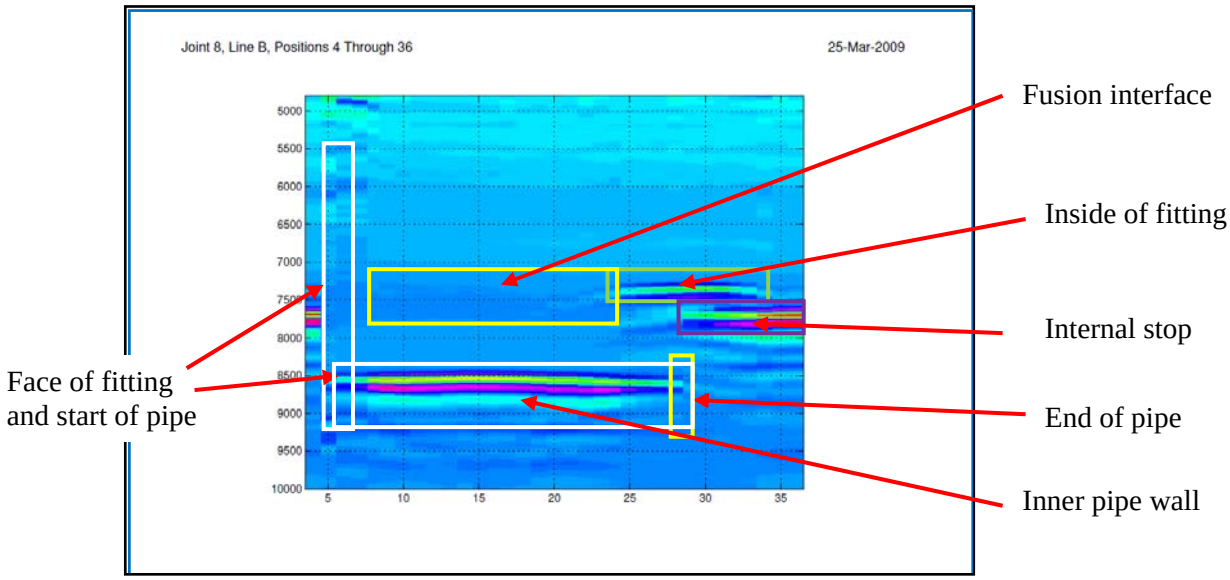

Figure 12: D-scan showing diagnostic areas of a non-EF fusion joint

Figures 14 through 21 show D-scans illustrating some of the flaws detected with automated analysis. In some cases, excess material is pushed past the pipe wall as illustrated in Figures 9 and 13. Figure 14 is a D-scan showing the detection of bead that extends past the inner pipe wall. Signal peaks such as those in the white box in Figure 14 are not present in Figure 12, demonstrating the ability to access the amount of material at the end of the pipe. One might expect that the distribution of material at the end of the pipe is not an issue as long as the rest of the fusion is good. However, it is known that excess material can create stress risers causing the socket fusion fitting to fail with time when the joint is loaded. The ultrasonic inspection technique detects this material. It is beyond the scope of this project to determine the relationship of this material and field failures.

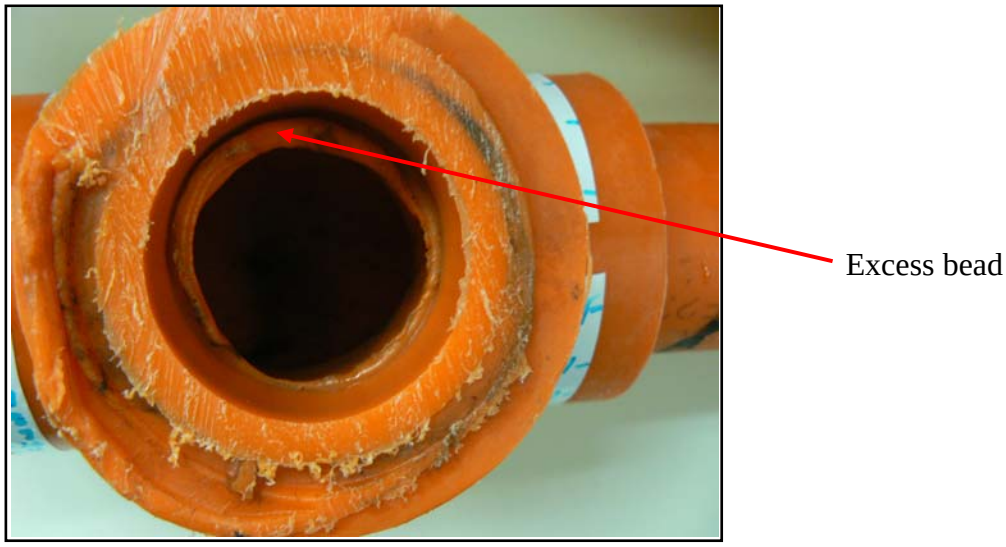

Figure 13: Photograph of excess bead inside socket tee

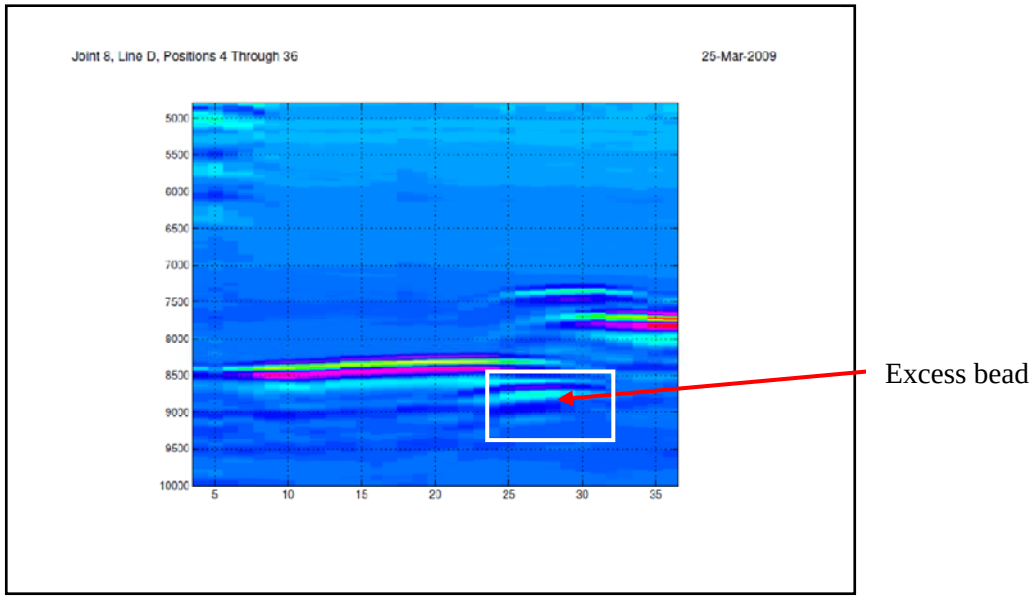

Figure 14: D-scan of socket fusion coupling with excess bead

For socket fusion couplings and tees, the waveform generated at each discrete sensor location is analyzed to identify voids and cold fusion. Additional information is required to assess the quality of the joint: specifically, is the length of pipe properly inserted and fused correctly? One flaw is "short stabbing" or not inserting the pipe the proper distance into the coupling. The length of the pipe inserted into the fitting is compared to the accepted value. Figure 15 is a D-scan where the pipe was prevented from being fully inserted. The incorrect insertion length is detected because the pipe length is short and because the reflections from the back wall are reduced. It is also possible to detect pipe that has been inserted too far into the fitting.

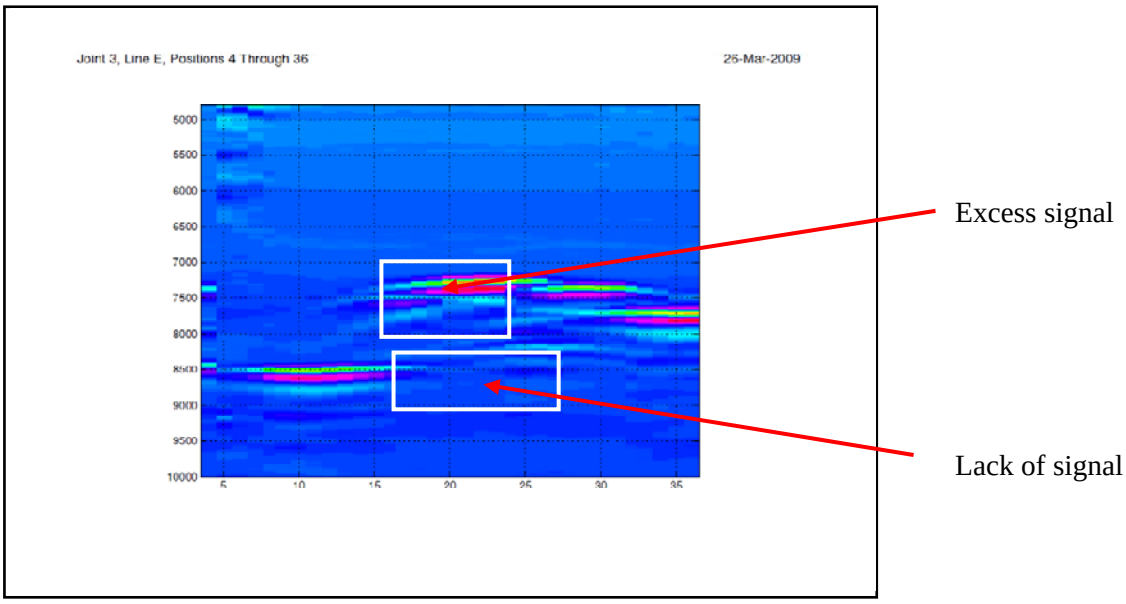

Figure 15: D-scan of non-EF coupling where the pipe was short stabbed

Figure 16 shows the D-scan of a joint made with a coupling that was pre-drilled with a 0.092-inch (2.3 mm) diameter bit before the joint was made. The size of the hole in the D-scan (white box) appears larger than its actual size because of the finite size of the sensor. As the sensor is scanned, the front edge of the sensor detects reflections from the top of the hole. The hole continues to be detected until all of the sensor passes over the hole. Because the hole is smaller than the sensor, the amplitude does not change greatly during the passage. Note the corresponding reduction in signal strength (yellow box) from the inner pipe wall because the hole reduces the amount of ultrasonic energy reaching the wall. Figure 17 shows a D-scan of a different part of the same coupling with a V-groove cut across the coupling. The V-groove simulates a deep scratch and the drill hole a void. Both are clearly detected.

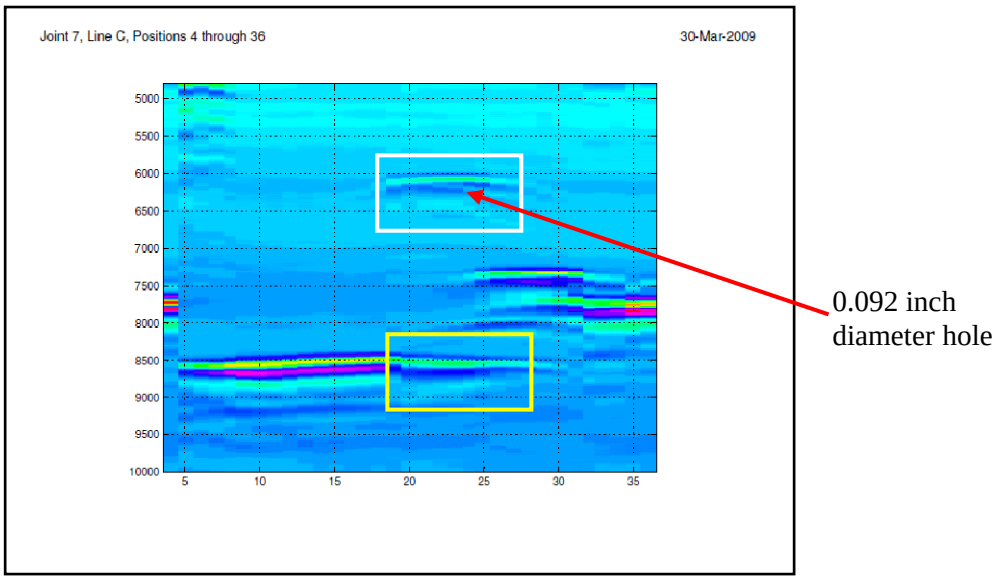

Figure 16: D-scan showing a 0.092 hole in the coupling

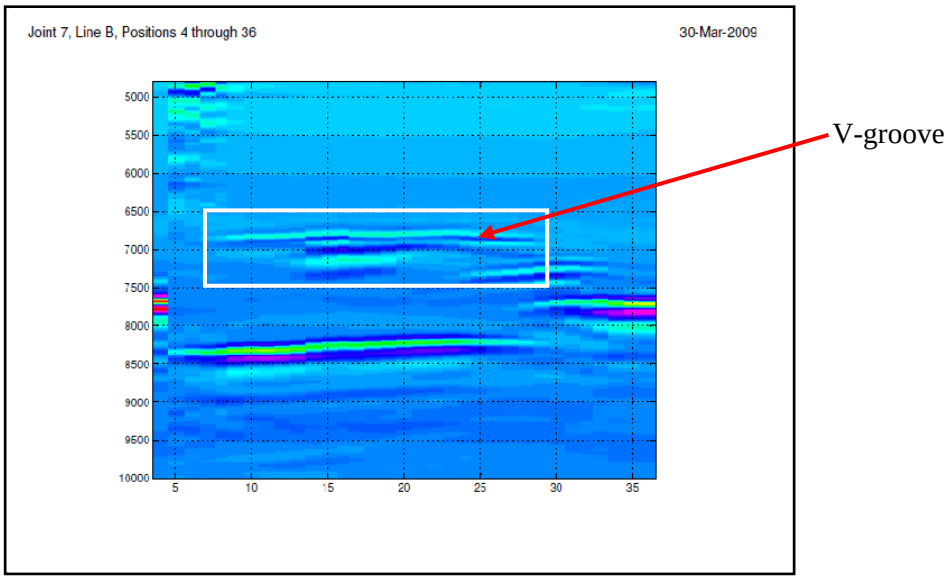

Figure 17: D-scans showing V-groove in the coupling

The butt fusion analysis approach was adapted for the 2-inch PE 2306 socket fusion couplings by making the appropriate model to select the independent parameters and making measurements to obtain the dependent parameters. The model was applied without changes to the orange 2-inch socket tees. Figure 18 shows the location of a leak on a socket tee. Figure 19 is a D-scan showing the existence of the leak. There is a crack in the pipe wall and lack of fusion from the front of the coupling to the crack. The complete lack of fusion is shown by no reflection from the inner pipe wall. In addition, there is poor fusion from positions 11 through 18 as shown by the existence of some signal at a depth of 7400 to 7700 and reduced amplitude in the reflection from the inner pipe wall.

Figure 18: Photograph of tee showing location of leak

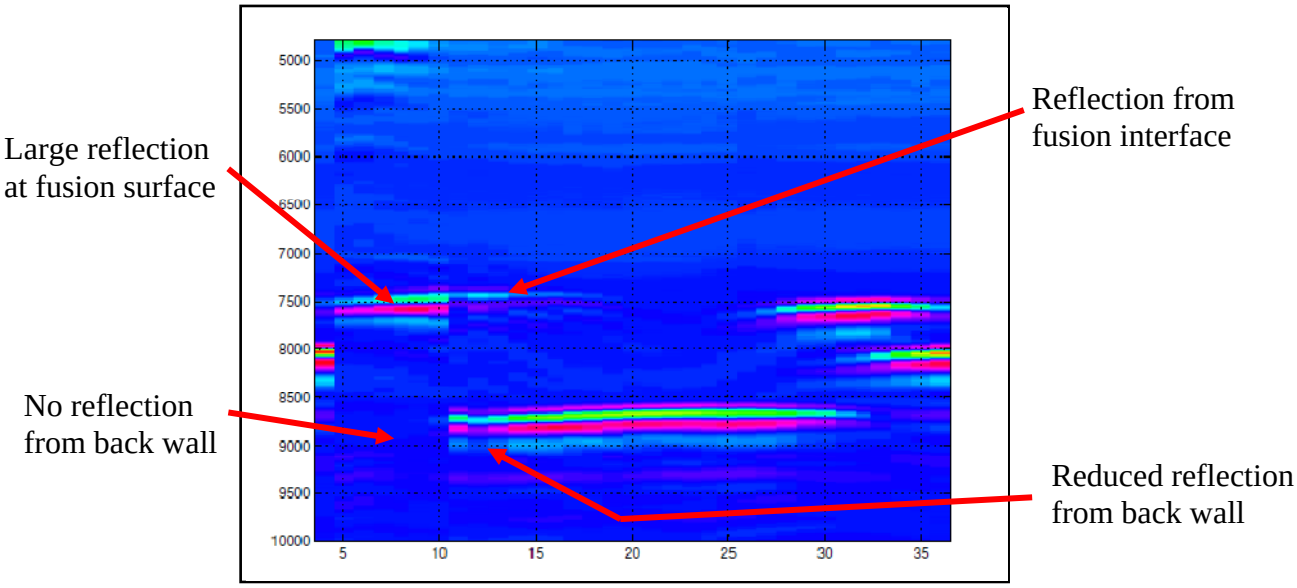

Figure 19: D-scan showing a leak in a socket fusion tee

Figure 20 shows an overview of the same tee as Figure 18. The crack is on the left side of the tee facing away from the reader. D-scans were also made on the right hand side of the tee. Figure 21 is a D-scan taken along the bottom of the left hand side of the tee. Incomplete fusion is shown at the interface (white box) between the tee and the pipe. Note that there is still a strong reflection from the inner pipe wall, unlike in Figure 19 where there is complete lack of fusion. There is also a slope in the signals from the inner pipe wall relative to the x-axis, which will be explained in the next section.

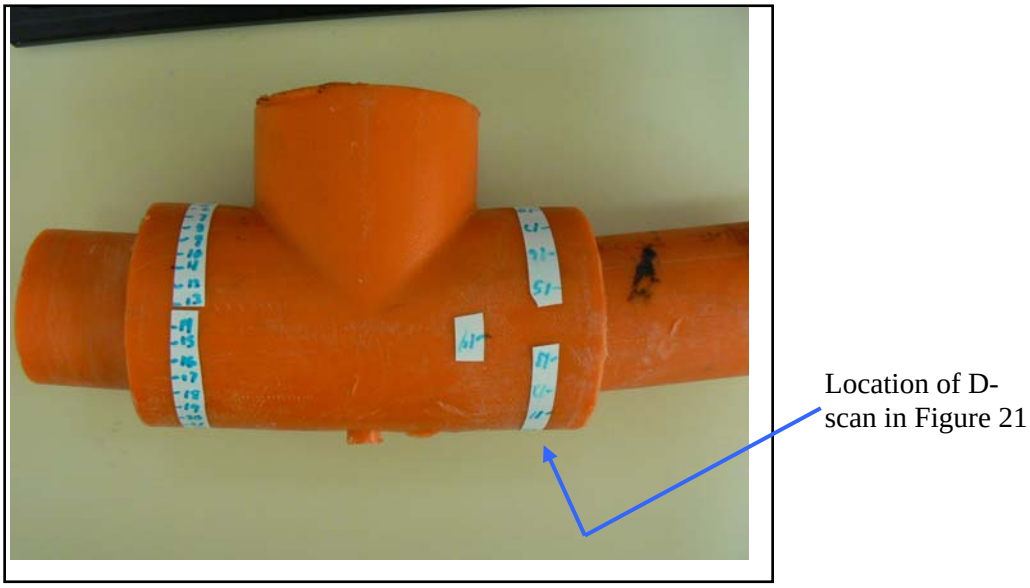

Figure 20: Photograph of pipe inserted at an angle into a tee

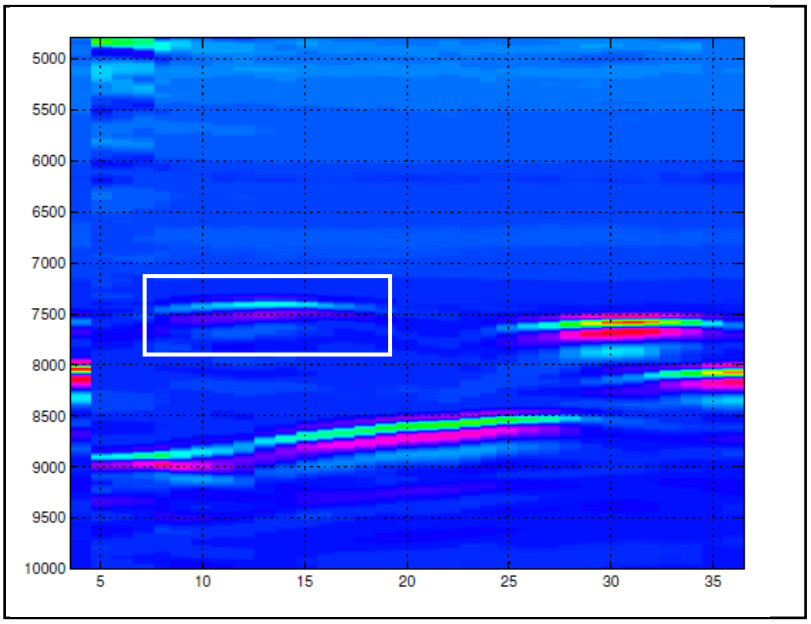

Figure 21: This D-scan shows incomplete fusion

Measurement of ovality and angle of pipe insertion

Figure 22 is a D-scan collected around the circumference of a 2-inch fusion coupling. The horizontal axis gives the position of the sensor on the circumference. The sensor was shifted 4 mm in each step, with 64 steps covering 360°. The vertical axis is proportional to the time required for a wave reflection from a flaw or boundary in the fitting/pipe. Signals between 0 and 4850 are not shown because they are in the stand-off and do not assess fusion quality. If the pipe were centered in the fitting and had 0% ovality, the yellow, red, and green lines would be parallel to the x-axis. The sinusoidal variation demonstrates that the pipe is oval or inserted at an angle.

A second circumferential scan will determine which is correct. Figure 23 is a schematic illustrating a pipe inserted at an angle (left side) and an oval pipe inserted at the correct angle (right side). The dotted lines on Figure 23 show the positions of the two circumferential scans. If, as illustrated on the right side of Figure 23, the pipe is oval, the two scans would have maximums and minimums at the same position. If, as illustrated on the left side of Figure 23, the pipe is at an angle, the maximums and minimums would reverse: at the top of the joint the thickest measurement is at the black dotted line and the thinnest is at the red dotted line. Figure 22 also shows the presence of three holes made in the coupling and that where in the path of the circumferential scan.

Currently there is a standard which rejects joints where the ovality exceeds 5%. There is not a standard in terms of an angle of insertion. However, it is known that pipe inserted at too large an angle can result in failure, such as in Figure 21. It is beyond the scope of this project to develop a standard for angle of insertion. A combination of ovality and insertion at an angle can also occur. It is possible to fit the data from the two circumferential scans to an equation describing the cross section and determine the amount of ovality and angle of insertion.

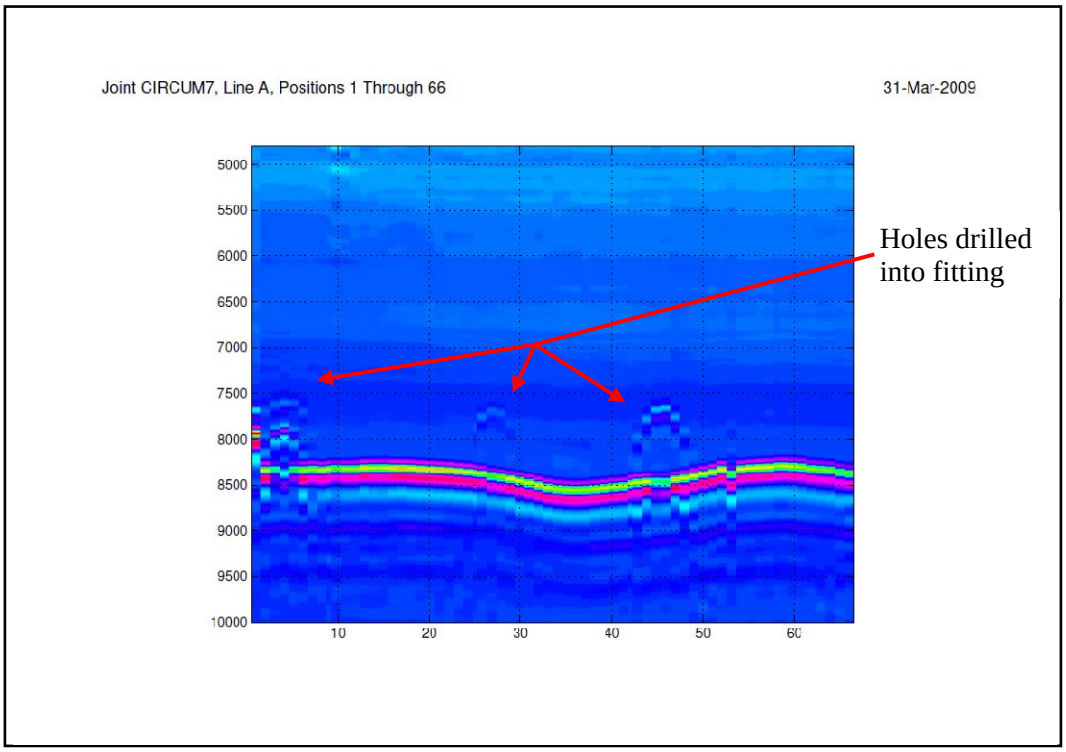

Figure 22: Circumferential scan showing the pipe is at an angle or is oval

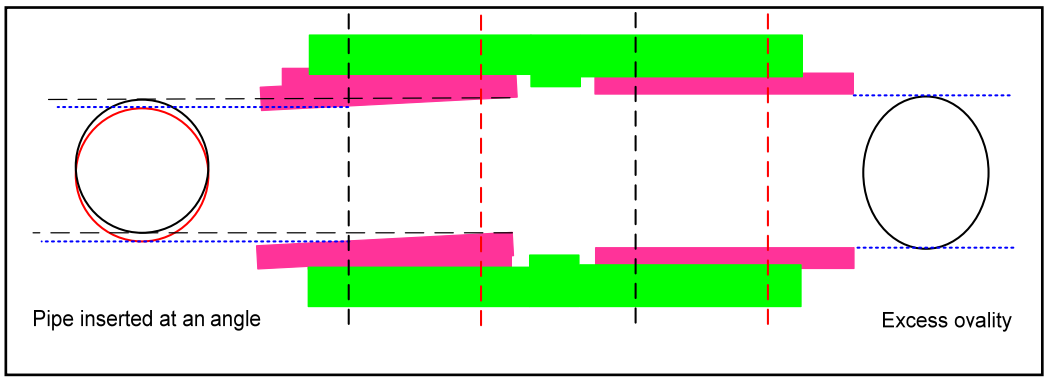

Figure 23: Schematic of a joint made with a pipe inserted at an angle and an oval pipe

Non-EF Saddle Tees

Scan patterns for non-EF saddle tees

Scan patterns and stand-off/wedge designs for saddle fusion tees present a challenge because of the large number of saddle tee shapes. The geometries of saddle fusion tees vary with manufacturer in terms of diameter of the main being fused to the tee, diameter of the outlet pipe, and the heights of the bases. Part of the fusion surface is below the body of the fitting, restricting access to inspection of that part of the joint. The curvature of the some base tops is not concentric with the center of the pipe. This means a pulse/echo sensor placed on top of the base will not receive a direct reflection from the fusion interface. Figures 24 to 26 show sample variations in the saddle tee bases. All of these tees were fused to 2-inch diameter MDPE pipe. Figure 24 shows a saddle tee design where the side of the rectangular base is flat and the base extends away from the body of the tee. This provides access for sensors. Figure 25 shows a tee where the base is smaller and curved and the bead restricts placement of the sensors. Figure 26 is the third example showing the base underneath the connection to the service line. The connection to the service line restricts the height of the scanning mechanism.

As with the other joints, the best quality assessment will occur if the entire fusion interface is inspected. In addition, an automated inspection system must require minimal input from the operator on the position of the sensor. Several sensor/scan geometries were investigated for saddle tees with the above criteria in mind. The geometries included placing the sensors on the body of the pipe, rather than on the saddle tee. GTI did not find an arrangement where sufficient ultrasonic energy returned to the sensors in either the pulse/echo or pitch/catch modes to permit complete inspection of the fusion area. GTI concluded that in spite of the drawbacks, the sensors must be placed on the tee itself.

Not all of the fusion surface can be inspected ultrasonically. One issue that must be determined in future work is whether or not the limited portions that can be inspected provide enough information to correctly assess joint quality.

Figure 24: This rectangular base permits access for inspecting the fusion area

Figure 25: The curved base creates challenges for inspection of the fusion area

Figure 26: The service tee restricts the height of the scanning mechanism

A combination of two sensor geometries can be used to inspect saddle tees with bases having flat surfaces parallel to the axis of the pipe. In the geometry shown in Figure 27, sensors are placed on each side of the tee. Pitch/catch ultrasonic signals are sent across the tee base through the crown of the pipe with imperfections in the fusion interface scattering signals and reducing the detected signal. For some tees whose geometry is similar to that in Figure 27, the fusion interface (shown in red) can be inspected by moving the pair of sensors along the two flats parallel to the axis of the pipe.

In cases shown in Figure 28, where the distance between the lowest edge of the fitting and the crown of the pipe is greater than the pipe wall thickness, the sensor placement geometry shown in Figure 28 misses parts of the fusion area. To inspect those parts, a complex wedge is required as shown in Figure 29. Each tee geometry requires a custom wedge. Two sensors are mounted on the wedge. The wedge is designed so that the axis of each sensor passes through the center of the pipe. Each sensor is used in pulse/echo mode (as illustrated by the red and green arrows in Figure 29) to inspect the area directly beneath it. The pair of sensors is used in the pitch/catch mode to survey the fusion interface not directly under either sensor (as illustrated by the blue arrows).

The stand-offs shown in Figures 27 and 28 are used to avoid irregularities in the signal caused by the initial impulse to the sensor. Their thickness must be chosen to prevent multiple internal reflections within the stand-off obscuring inspection of desired features. To collect additional information, the pitch/catch roles of the sensors are reversed: the same analysis algorithm is used. For designs such as Figure 29, the thickness and shape of the wedge must be designed to minimize interfering reflections.

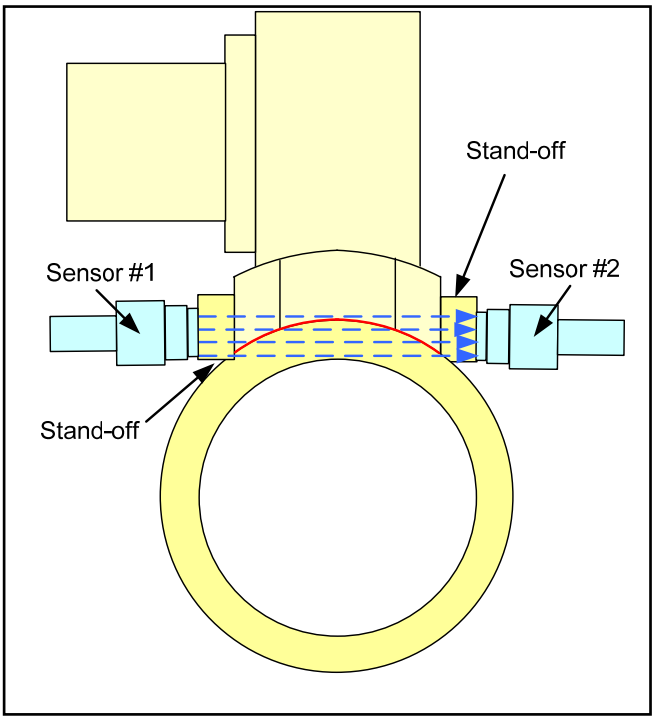

Figure 27: Tees with sufficiently narrow bases can have the fusion area (red line) inspected

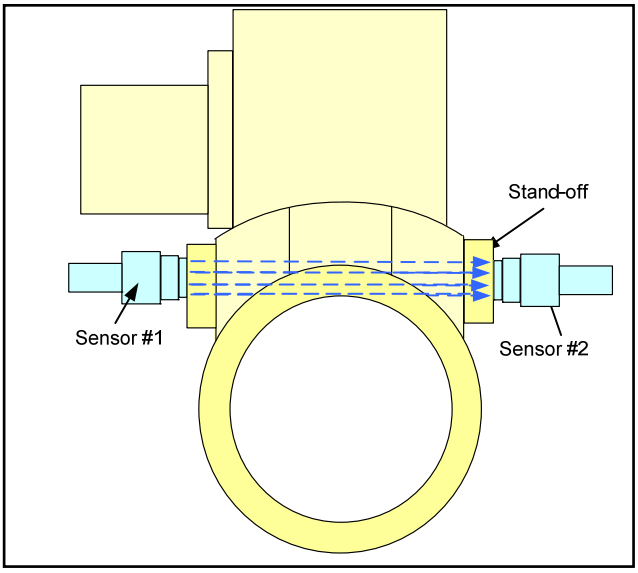

Figure 28: Tees with a broad base require additional sensors to inspect the joint

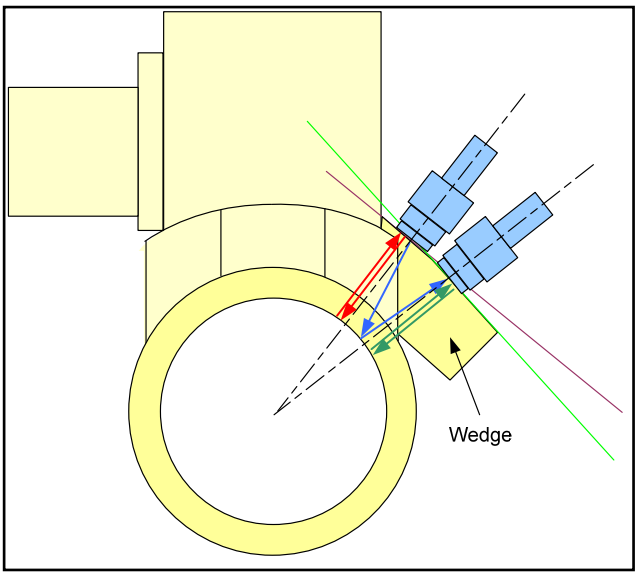

Figure 29: A complex wedge is required for tee geometries in Figure 28

Detection of flaws in non-EF saddle fusion tees

A series of non-EF saddle tees joints were made with yellow US Poly UAC 2000 4-inch IPS SDR 11.5 pipe. The fittings are Central Plastics 10005981 4-inch IPS pipe, 1-inch IPS service tee yellow PE2406. Figures 30 and 31 show the process of making non-EF saddle fusions. Dirt on the pipe is removed with an alcohol wipe. Then the pipe and bottom of the tee are roughened with 50 grid sandpaper supplied with each tee, followed by wiping with clean, dry paper cloth. As per manufacturer's instructions, no alcohol wipe was used after sanding the pipe and fitting. The tee is test fit to the pipe to ensure proper alignment—with 100 psig pressure used to seat fitting. The manufacturer's recommended fusion temperature of 500 ^{o}F $\pm$10°F for 40 seconds and a pressure of 80 psig pushing the fitting onto the heating iron were followed. After the heating iron was removed, the fitting was pressed against the pipe with an initial pressure of 70 psig. This pressure quickly decreases as the joint cools.

When the joints were made, the plastic welled up higher on some of the joints than expected (See Figure 32). GTI elected to remove this excess material from all of the joints (Figure 33). Although not desirable in field operation, this permits development of techniques to detect flaws. A mechanism, shown in Figure 34, was designed and built to hold two sensors against the base of the saddle, following the scanning pattern in Figure 27.

Figure 30: The pipe and saddle tee are heated simultaneously

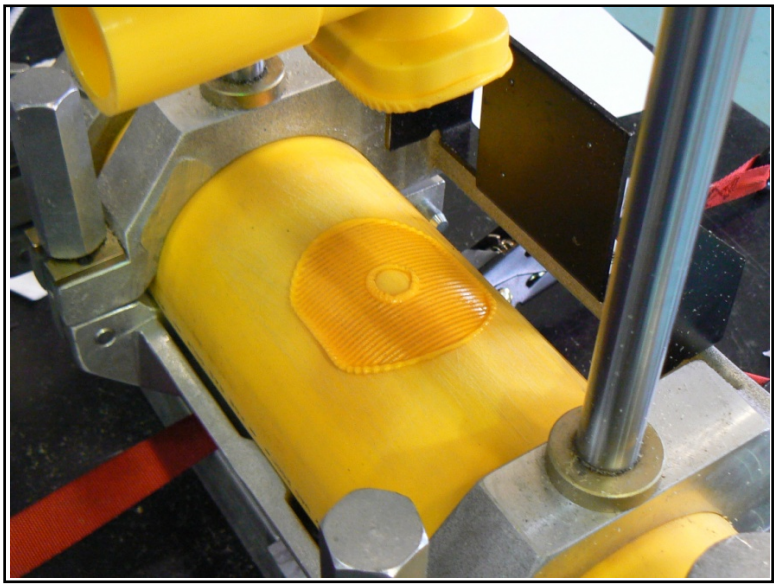

Figure 31: The iron creates a rippled surface on the pipe and tee

Figure 32: Completion of a non-EF saddle fusion joint with excessive bead roll back

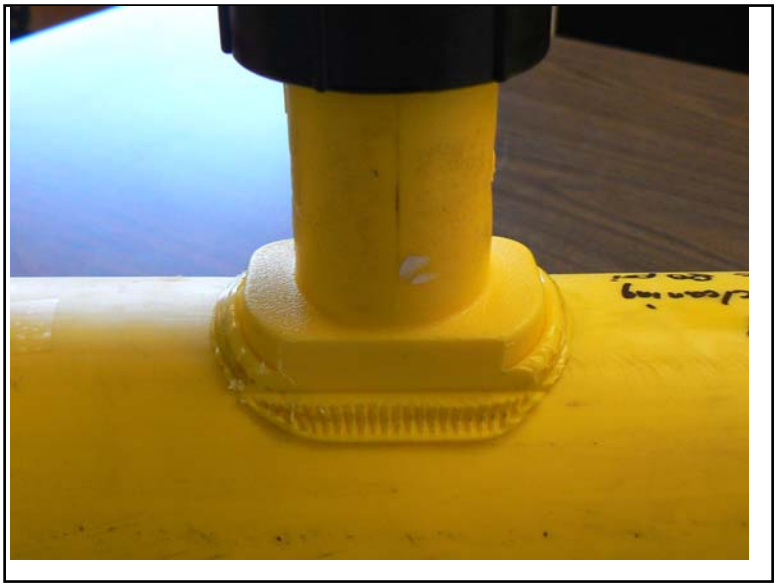

Figure 33: Same saddle fusion joint with material removed

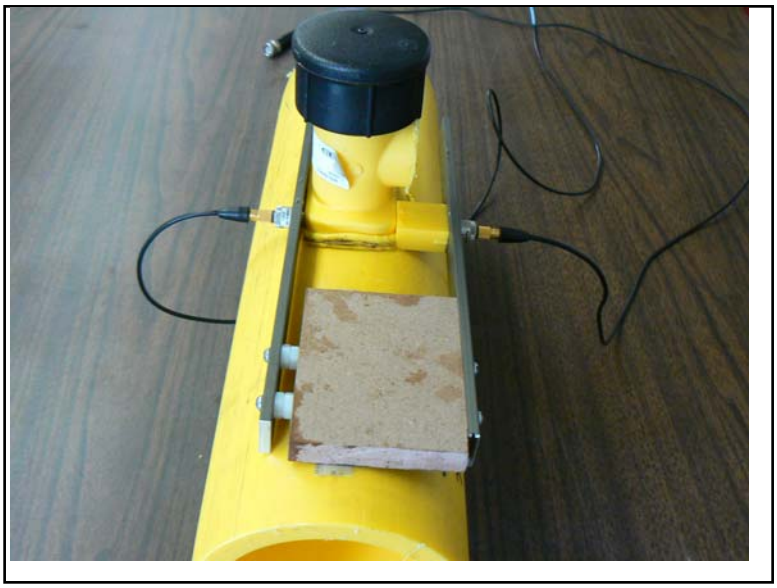

Figure 34: Photograph of mechanism to collect data on the non-EF saddle tees

Detection of flaws in non-EF saddle fusion tees

Figure 35 shows a D-scan from a non-EF saddle tee made following the proper procedures. The feature across the D-scan at 2900 is the reflection from the stand-off/fitting interface. The features in the white box are reflections from the center hole of the saddle tee. (When the saddle installation is completed, gas flows through the center hole.) As with other features, the diameter of the sensor makes flaws and features appear larger than their physical dimensions. Figure 36 is the D-scan of a joint with two 1/8-inch diameter holes drilled into the saddle tee. The drilled holes are in front of the center hole of the tee. The white and yellow boxes show the drilled holes.

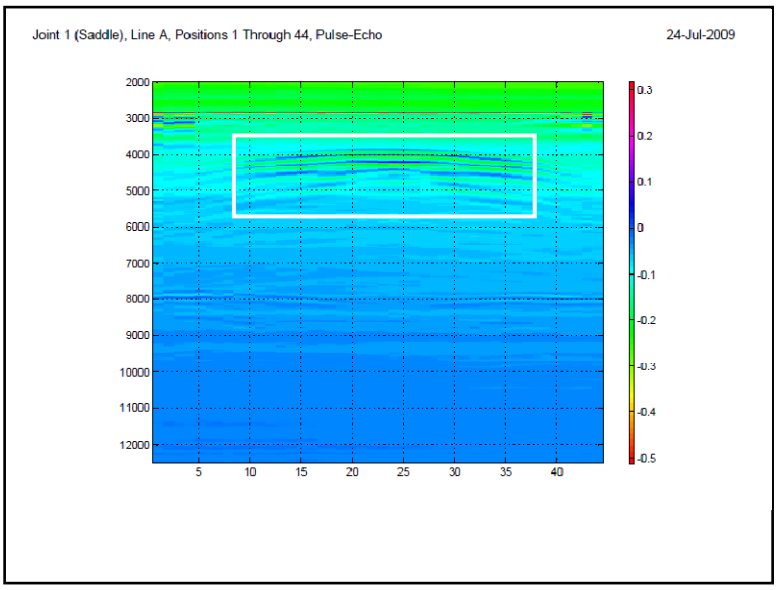

Figure 35: Pulse/echo D-scan for properly made non- EF saddle tee

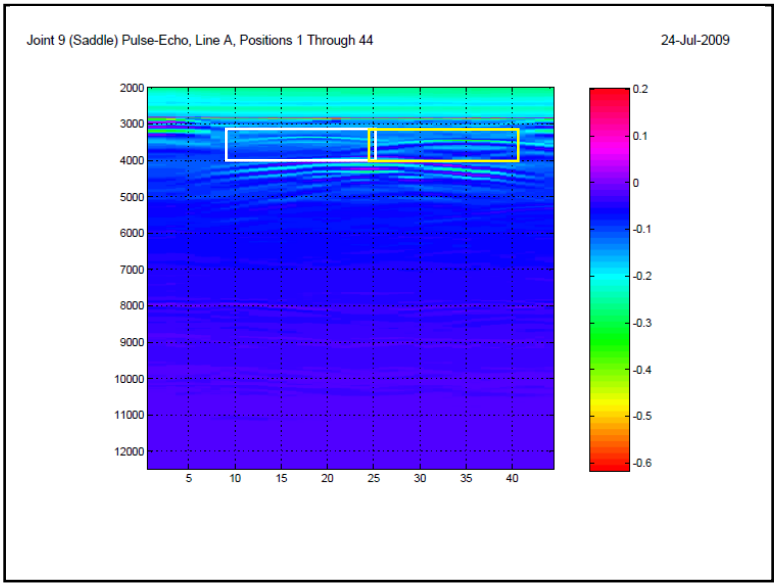

Figure 36. Pulse/echo D-scan for non- EF saddle tee with two 1/8-inch holes

Figure 37 shows the pitch/catch D-scan from a non-EF saddle tee made following the proper procedures. The feature across the D-scan at 3900 is the arrival of the ultrasonic wave from the transmitter sensor. The two white boxes highlight the location of the analysis areas. Each white box has three zones that are tested separately. The first zone is the amplitude of the initial signal arriving from the transmitting sensor. The amplitude of this part of the signal is decreased with poor quality fusion. The next zone gives the amplitude of waves that reflect from the fitting/pipe interface to the top of the fitting, back to the interface and to the sensor. The third zone has three reflections. Figure 38 shows the paths. Poor quality fusion increases the amplitude of these waves. The portions of the D-scan at positions 5 to 9 and from 35 to 39 are those least effected by curvature at the ends of the tee base and by the center hole of the tee.

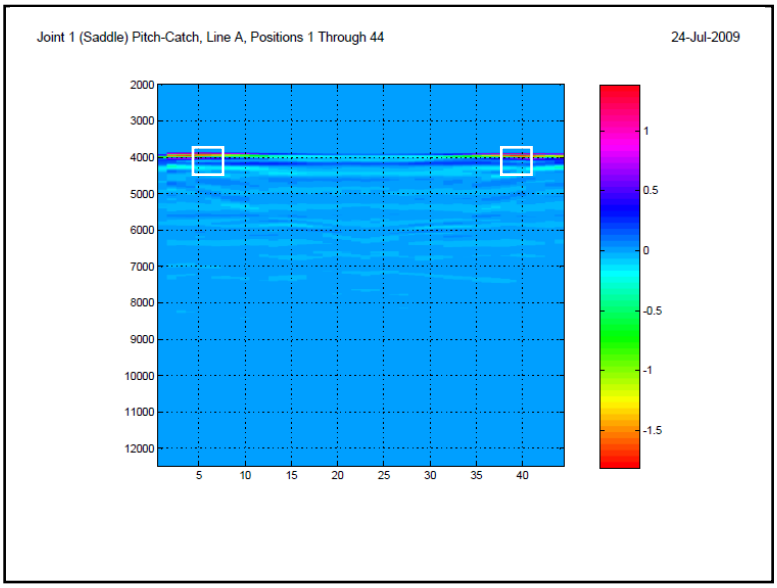

Figure 37. Pitch/catch D-scan for a properly made non- EF saddle tee

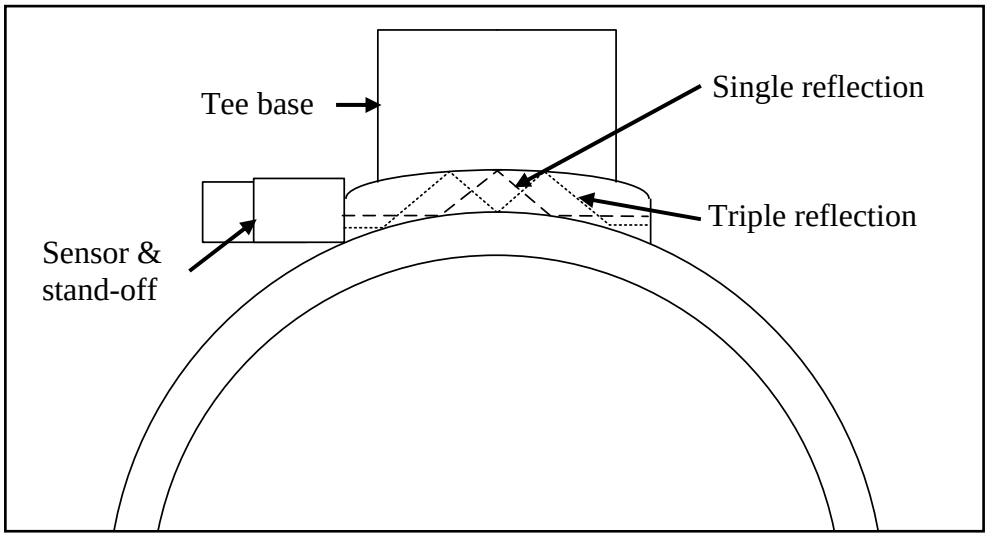

Figure 38. Schematic of selected paths in non-EF saddle tee

EF Socket Fusion Couplings and Tees

Scan pattern for EF couplings and tees

Figure 39 is a photograph of a 4-inch diameter EF coupling with the sensor/stand-off used. Figure 40 is a schematic of the recommended scan pattern. The EF coupling has a ridge in the center of the coupling. The coupling also has a sloped portion in which the total thickness of the fitting plus pipe decreases as the edge of the fitting is approached. There are no EF wires in the area under the ridge and the far ends of the coupling. Thus no fusion occurs there.

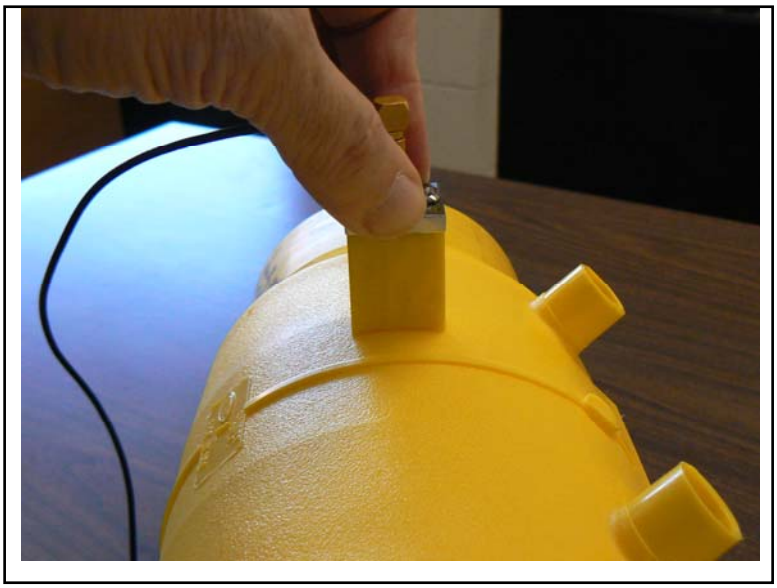

Figure 39. Photograph of EF socket fusion coupling with sensor and stand-off

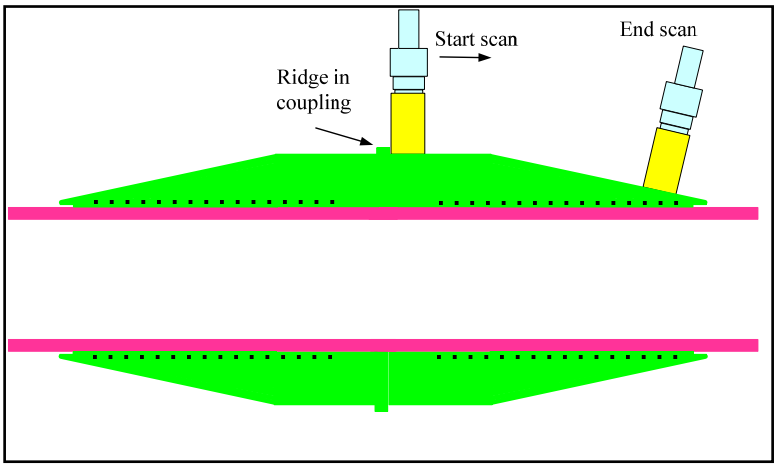

Figure 40: Scan pattern for EF coupling inspection

GTI recommends that data collection for the EF couplings use a single sensor mounted on a stand-off. A mechanical device should be designed to scan ½ of the coupling. The sensor is oriented perpendicular to the fitting and data is collected in pulse/echo mode. As illustrated in Figure 40, the scan motion is parallel to axis of pipe, starting with the sensor at the ridge in the coupling. The sensor is moved collecting data at each step, until the center of the coupling is reached. GTI elected to use 1 mm steps, which is one eighth of the diameter of the sensor. After a scan parallel to the pipe axis is completed, the sensor is returned to the starting position. Next the sensor position is incremented around the circumference and another scan parallel to the pipe axis is performed. The process of scanning axially and incrementing circumferentially continues until the entire fusion interface is surveyed. The EF coupling has a "flat" portion where the coupling is concentric with the pipe and a "sloped" portion where the coupling forms a cone. The differences in radii of the coupling in the EF coupling are sufficiently small that the same wedge can be used. The "pebbly" outer surface of the EF coupling (compared to the smooth surface of the pipe) requires careful application of couplant to fill the voids. To inspect the second half of the coupling, the mechanism is removed and placed on the opposite side. EF couplings have protuberances and raised labels. These need to be removed in order to inspect as much of the joint as possible.

The ovality of the coupling/pipe and the angle of insertion of the pipe into the fitting can be measured after the joint is made. That determination requires data from two circumferences around each end of the fitting. This data can be obtained from the axial scans data at the appropriate positions. Alternatively, two scans can be made by moving the sensor in steps around the circumference of the fitting. As with the non-EF couplings and tees, a single sensor proved to be a better choice than the pair of sensors on wedges used for butt fusion inspection.

Detection of flaws in EF couplings

Nine 4-inch diameter EF coupling joints made with MDPE US Poly UAC 2000 4-inch IPS SDR 11.5 yellow pipe. All but one of the joints was made with yellow MDPE couplings from Central Plastics 4-inch IPS, PE2406 model number 5757008. The black HDPE coupling is a Central Plastics 4-inch IPS, PE3408/PE4710 model number 10000360. The pipe surfaces were wiped and then scraped to remove the surface layer. Manufacturer's instructions for both couplings call for 40 volt, fuse for 200 seconds, cool for 15 minutes.

Figure 41 is a D-scan of a good EF coupling fusion. The D-scan has three obvious features identified by the red arrows: Reflections from the stand-off/coupling interface, reflections from the EF wires, and reflections from the inner pipe wall. The upper line is parallel to the x-axis because the height of the stand-off is constant for all of the measurements. The line for the EF wires starts parallel to the x-axis and then slopes upward at position 25 which corresponds to the start of the slope in the coupling. The coupling thickness is thinner at the end; therefore, the travel time of the ultrasonic wave is less. The positions of reflections from the inner pipe wall are more complex and are due to the shape of the coupling and distortions in the coupling/pipe. The latter is shown in the photograph in Figure 42; where because of the thermal expansion and construction in the coupling and pipe, the inside surface of the pipe wall is no longer flat after the fusion is complete. The white, yellow, and orange boxes identify zones in the D-scan used to help classify joint quality.

Figure 43 is a D-scan of a joint with a 38 by 22 mm, 0.010 inch thick piece of aluminum tape inserted between the coupling and pipe to simulate complete disbondment. Reflections occur from the sheet just below the EF wires. Very few ultrasonic waves pass through the tape and, thus, there is no detectable reflection at the inner pipe wall.

Figure 44 is a D-scan of a joint where three disks (4.7, 2.0, 2.4 mm diameter) of 0.010 aluminum tape were attached to the properly prepared pipe wall before the pipe was inserted into the coupling and fused.

The black squares show the positions of the disks. Arrows point to reflections from the 4.7 and 2.4 disks. There is no obvious reflection from the 2.0 mm disk. Figure 45 is a D-scan from a joint with a thin layer of dry dirt was placed on the pipe before the fusion. The red arrow highlights reflections from the dirt/coupling/pipe interface. In this case, the reflection is not total and there is reflection from the inner pipe wall. Figure 46 is a D-scan from a joint with a thin layer of mud on the pipe. The red arrow highlights reflections from the mud/coupling/pipe interface and the green arrow identifies loss of reflection from the inner pipe wall.

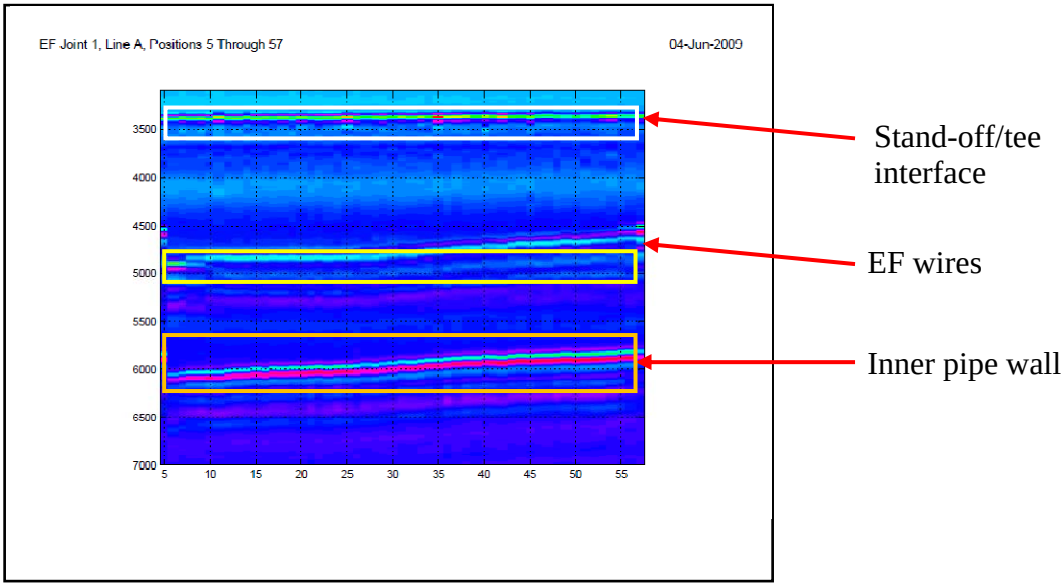

Figure 41. D-scan of 4-inch EF coupling made with the proper procedures

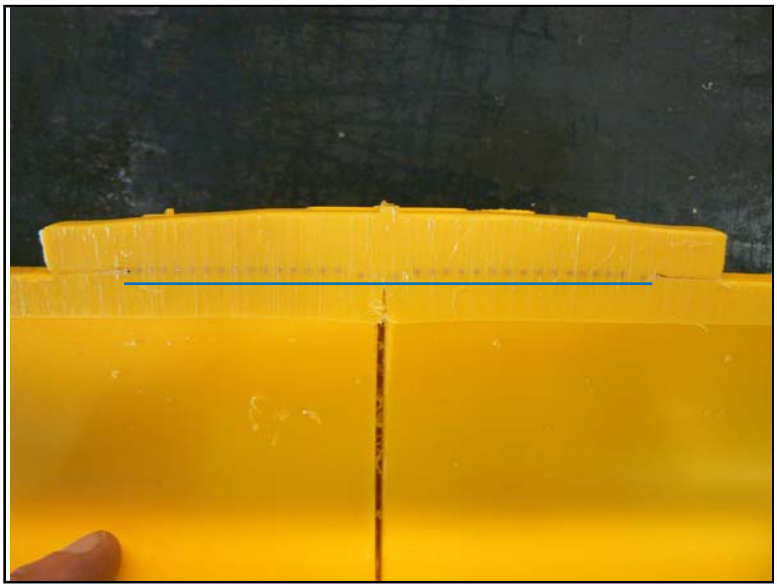

Figure 42. Photograph of normal distortion of the inner pipe wall caused by thermal effects

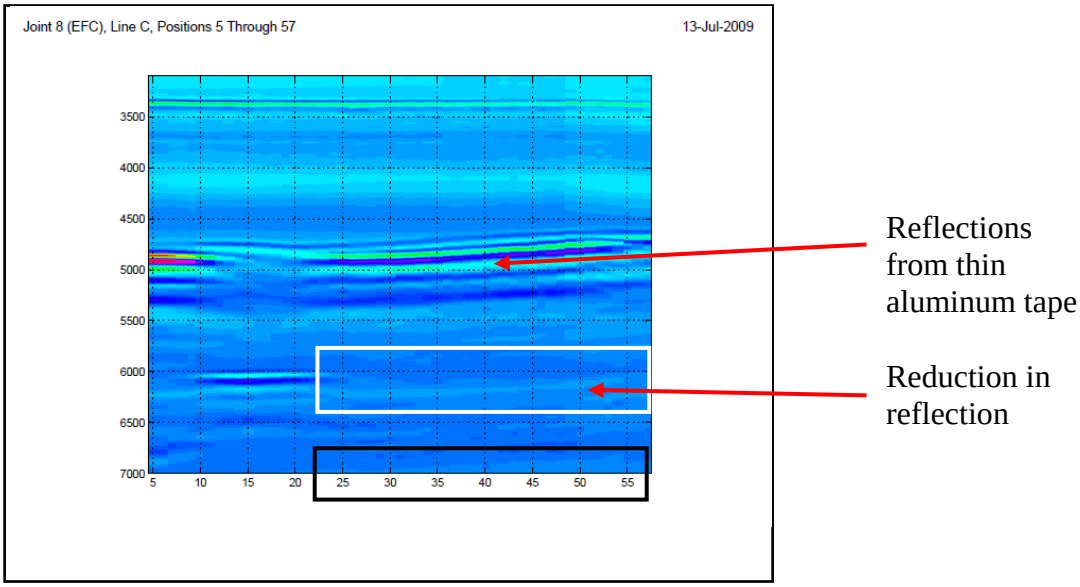

Figure 43. D-scan of 4-inch EF coupling for aluminum sheet located from position 25 to 57

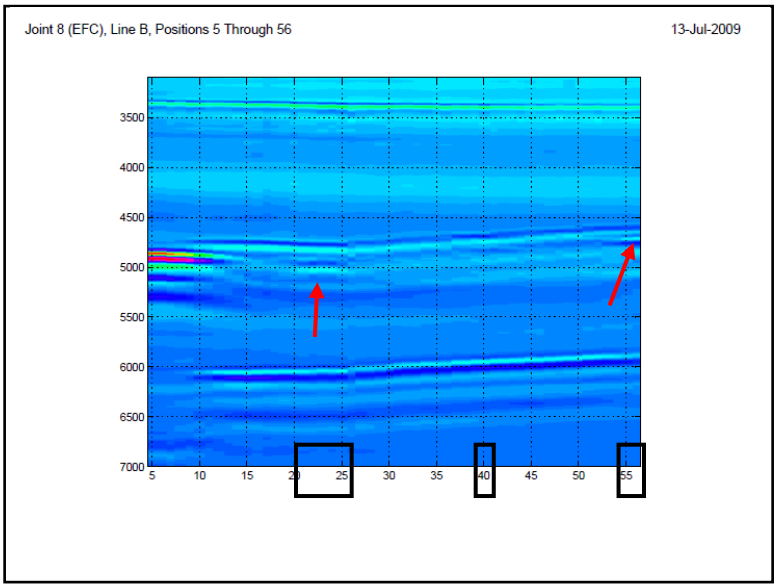

Figure 44. D-scan of 4-inch EF coupling with small aluminum disks 4.7, 2.0, and 2.4 mm

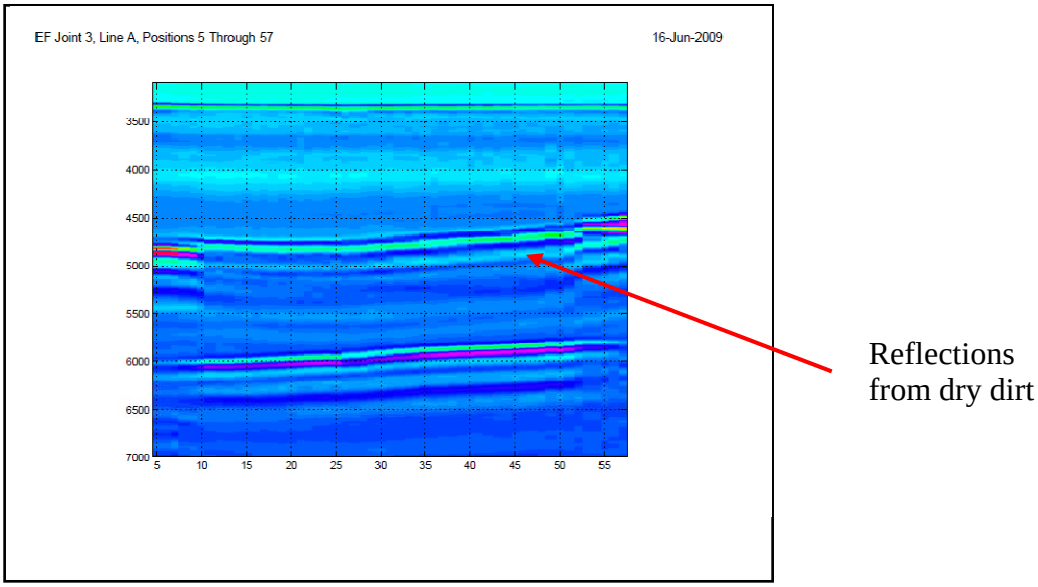

Figure 45. D-scan of 4-inch EF coupling with dry dirt

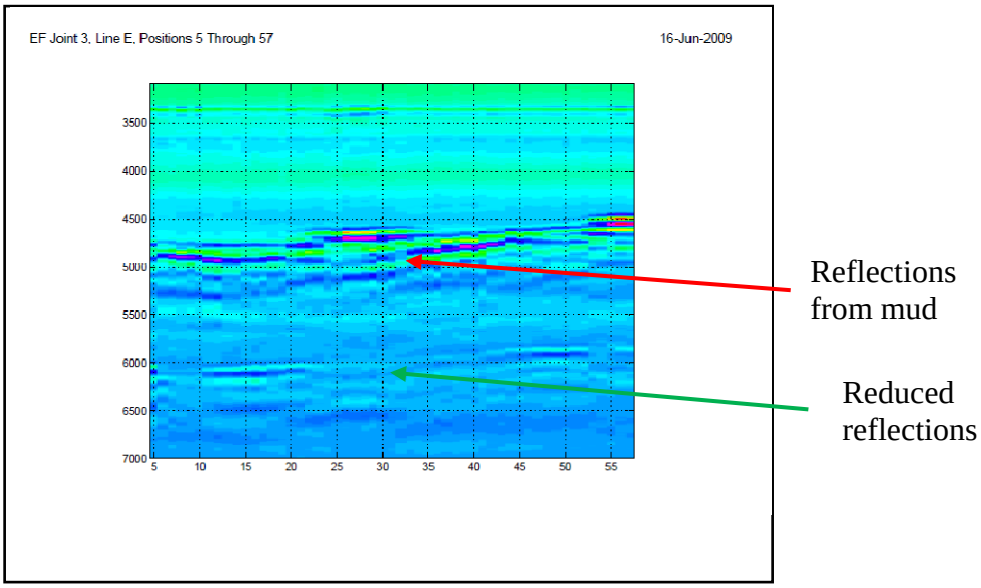

Figure 46. D-scan of 4-inch EF coupling with mud

EF Socket Fusion Couplings and Tees

Scan pattern for EF saddle tees

Figure 47 is a photograph of a 4-inch diameter EF saddle tee. The joints were made with MDPE US Poly UAC 2000 4-inch IPS SDR 11.5 yellow pipe and EF saddle tees from Central Plastics 4-inch IPS, PE2406 model number 5757763. The joint is made by scraping the pipe to remove dirt and the oxidized surface layer. The saddle is clamped in place, the fusion equipment attached, and the joint made. Figure 48 is a cut-away of an EF saddle tee demonstrating over half of the EF wires are under the body of the tee, making it difficult to test that portion of the joint. Figure 49 is a schematic of the recommended scan pattern. Data was collected every 6° apart, with the exception of under the ridge at the crest of the saddle. Figure 50 shows the sensor/stand-off used to collect data. It also shows the variation in curvature in the inspection area at the base of the tee. Care must be taken to ensure good coupling between the bottom of the stand-off and the surface of the tee.

Figure 47: Photograph of an EF saddle tee on a 4-inch diameter pipe.

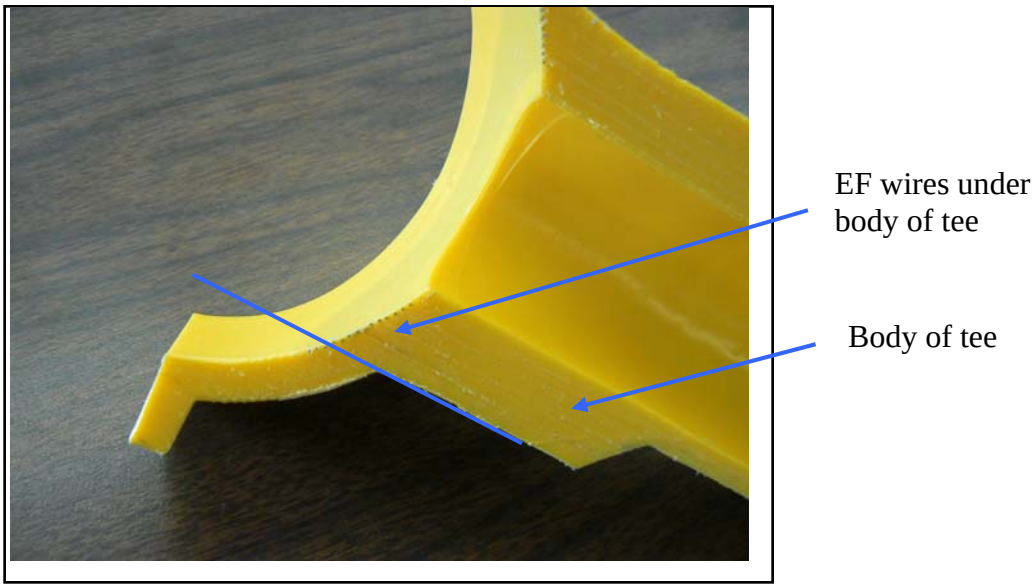

Figure 48: Single sensor arrangement for EF coupling inspection

Figure 49: Scan pattern for EF saddle tee inspection

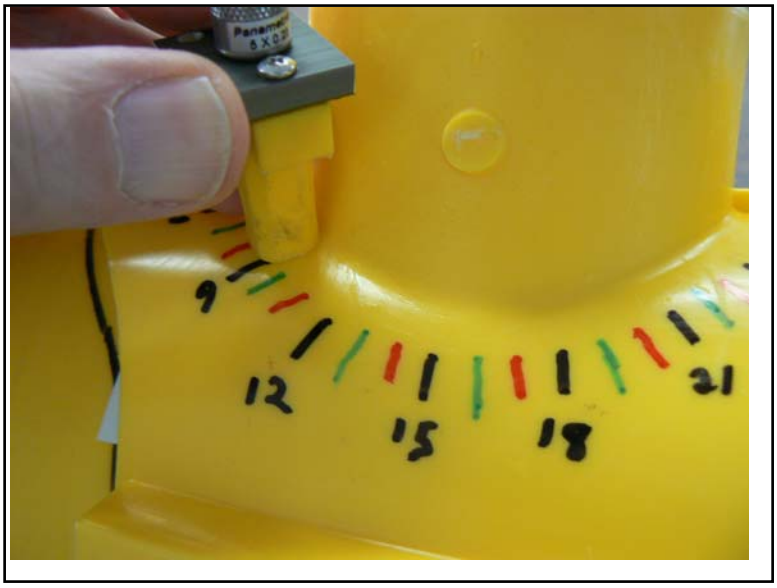

Figure 50: Sensor on stand-off for EF saddle tee inspection

Detection of flaws in EF saddle tees

Figures 51, 52, and 53 are D-scans for the EF saddle fusion tees. The joint in Figure 51 was made following the manufacturer's recommended procedure and was intended to be a good joint. The joint in Figure 52 was made with the proper procedure with two exceptions: a 1.45 by 8 inch by 0.020 inch thick piece of styrene plastic was placed between the pipe and saddle tee on one side and an oily glove was used to make a smudge on the opposite side. While these joints were made by the head fusion instructor at a local utility, in the next room operators were being trained in make EF fusion joints on 2-inch pipe. Although it was believed that correct procedures were being followed, two of these joints failed in destructive testing (See Figure 53). The class instructor repeated the process to make GTI a 4-inch joint. The D-scan for that joint is shown in Figure 54.

The D-scan in Figure 51 shows reflection from the EF wires and from the inner pipe wall. The red lines at positions 15 and 45 correspond to the lowest position on the coupling. There are probably no EF wires and thus no fusion at the very lowest part. Note that the reflections from the inner pipe wall are not parallel to the x-axis and form a regular pattern due to variations in the tee thickness. Figure 52 shows reflections at positions 9 through 23 from the styrene PE interface just below the EF wires and the corresponding strongly reduced reflection at the same positions from the inner pipe wall. This result would be predicted based on the location of the styrene. There are also reduced reflections (right-hand white box) from the inner pipe wall at positions 42 to 50, which correspond to the oil smudge. In Figure 53, the two white boxes highlight irregularities in fusion quality centered at positions 15 and 45, which correspond to the destruction failure locations of the 2-inch tees. The ultrasonic technique identified these flaws.

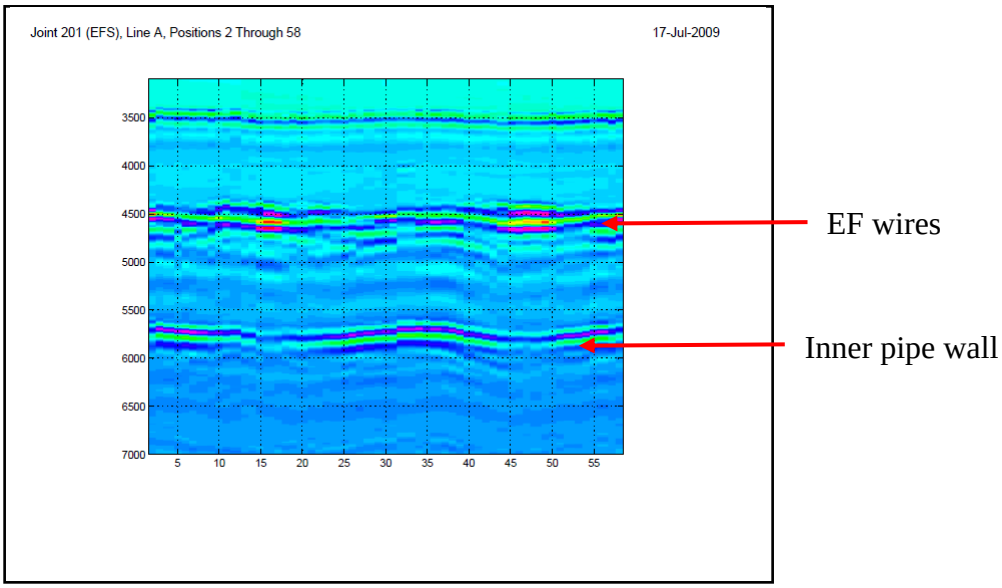

Figure 51: D-scan for a correctly made EF saddle tee

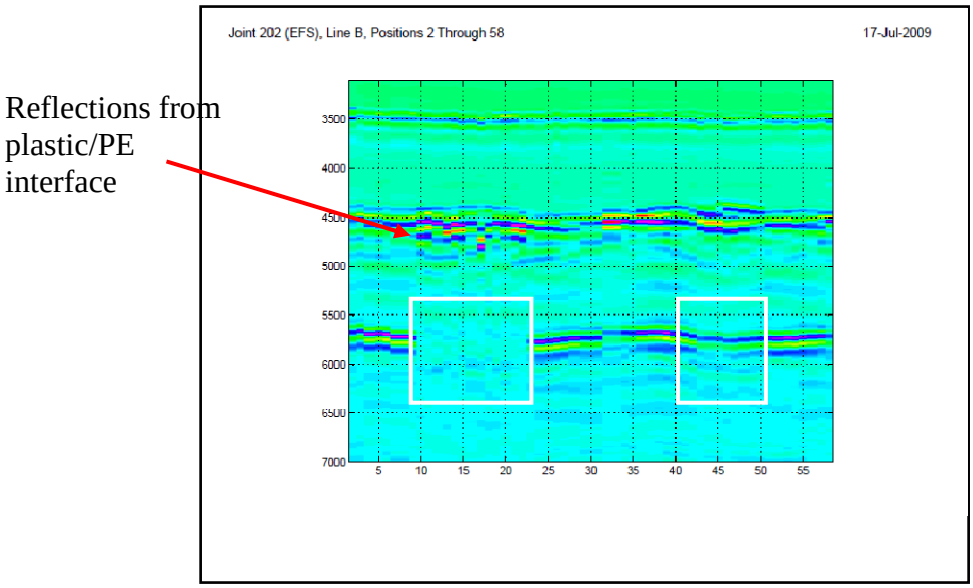

Figure 52: D-scan for an EF saddle tee with thin plastic insert and oily glove wipe

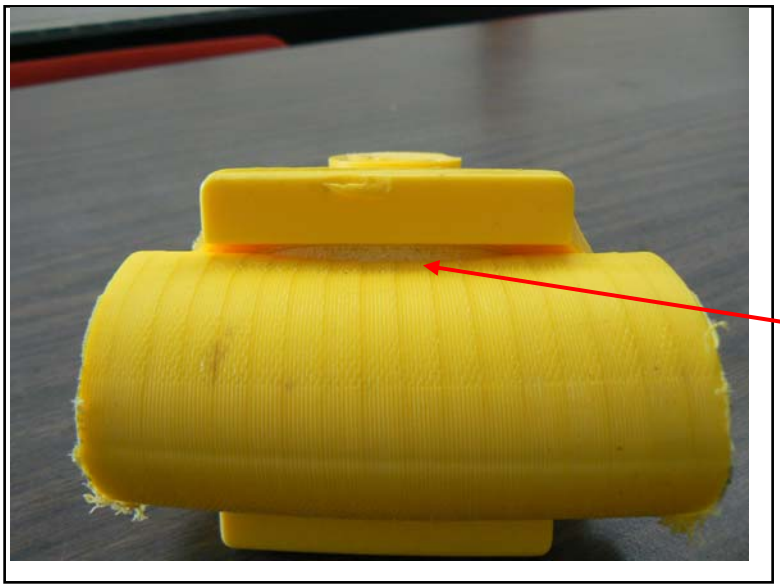

Figure 53: Photograph of failed 2-inch EF saddle joint

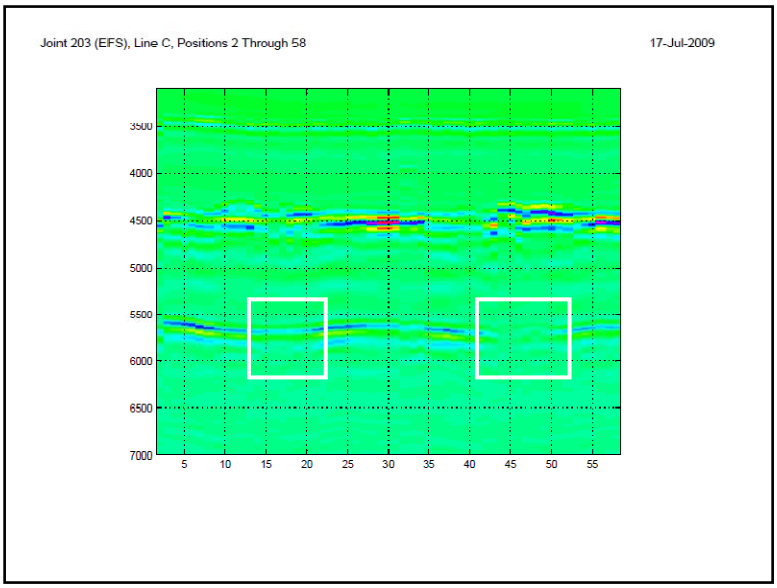

Figure 54: D-scan of EF saddle tee made similar to ones that failed

Results of the Automated Algorithms

Previous sections of the report gave the recommended scan patterns for the various fittings and examples of flaws that can be detected ultrasonically. The other portion of the project was development of algorithms to automatically discriminate good from bad joints with no input from the operator. As described earlier, the geometry of the joint and physical properties of wave propagation in the joint are used to determine independent parameters describing the fusion. Testing of good fusions is used to determine the dependent parameters. Samples of key zones are illustrated in previous figures. Several software algorithms were written; however, complete algorithms will require the addition of scanning hardware and the development of the control algorithms for the hardware. For example, collection and analysis of data require knowledge of the starting and ending points of the scan patterns. Development of hardware for non-EF couplings, tees, and saddle tees, and EF couplings and saddle tees was not part of this project.

The starting point for the analysis approach was developed in an OTD project (ref 18). The techniques correctly identified 53 of 53 flaws tested for.

All of the algorithms contain a test for insufficient couplant between the stand-off bottom and the top of the fitting. Proper coupling of the ultrasonic waves into the fusion joint under test is critical for a correct result. The most common couplant problem is not enough couplant. In such cases, too much of the wave is reflected at the stand-off fitting/interface and the reduced wave that propagates into the fitting gives incorrect results. In a field instrument, the first test would be for couplant quality and the instrument would add additional couplant and/or alert the operator to the problem.

The results of the automated analyses of the D-scans are given in Tables 1 through 4. Each table gives a number identifying the D-scan, the number of elements that did not meet the good joint criteria (number of failed elements, whether the joint passes (P) or fails (F), whether the prediction is correct (Y for yes and N for no), and a brief description of how the joint was made. The D-scans used to form the standard for the joint type are highlighted in yellow. The judgment of passing or failing is based on the introduced flaws. No destructive testing was performed to verify the quality of the joint. In some cases, GTI do not know if the way the joint was made is sufficiently bad to cause the joint to fail.

Table 1 lists the classification results for 34 D-scans of non-EF socket couplings. Six D-scans were used to determine the algorithm. The algorithm for this fitting generates two 27 element vectors that describe the quality of the joint. Each element can have the value -1, 0, or 1. All 54 elements must be 0 for the joint to be considered acceptable. Typically a poor joint fails more than one. D-scans 16 and 34 had insufficient couplant. Of the 34 automated D-scan tests, 31 gave the correct results including the six good D-scans and the two insufficient couplant scans. This includes tests for D-scans 30-34 where the fusion conditions were well out of specification. It includes D-scans 22, 23, and 25 where the fusion parameters are near the edge of what should reliably produce an acceptable joint. The fourth D-scan in this group (24) was assessed to be good. The other two, incorrect results (D-scans 18 and 19), were on the same joint that were intended to be good. The quality of this joint is not known and destructive testing is needed to determine the correct result.

Table 2 gives the results of the automated analysis of nine D-scans for the orange 2-inch diameter socket tees. These two tees were removed from the field because they had failed and were leaking. The algorithm for the yellow 2-inch couplings was used to assess the two tees. This is reasonable because the velocity of sound and attenuation of the yellow and orange PE2406 are similar. The automated algorithm failed all nine D-scans. The locations of the known leaks, the 5° angle of insertion of one of the pipes, visual inspection of the joints, and the large number of failed parameters strongly suggests this analysis is correct.

Table 3 gives the results of the automated analysis of eight D-scans for the yellow 4-inch diameter non-EF saddle tees. Two D-scans, 1 and 2, were used for the basis of a good joint. The automated algorithm gave 8 out of 8 correct predictions, including the two used as the standard.

Table 4 gives the results of the automated analysis of 34 D-scans for the yellow 4-inch diameter EF couplings. The automated algorithm gave 16 correct predictions, failed for 14, and 4 unknown. If proper procedures are followed, using a HDPE coupling with MDPE pipe will make a good joint. For D-scans 15 and 16 one element failed in the two scans, failing the one where both were expected to be good. Joints 16 through 20 were made with coiled pipe, with no effort to straighten the pipe. Not straightening the pipe is considered bad practice. However, the amount of curvature may not have been severe enough to cause failure. These four D-scans did not identify ovality or pipe inserted at an angle, thus the assessment of joint quality was given as unknown (??).

The results for the EF coupling assessments were mixed because of the slopes in the D-scans caused by the shape of the coupling and because of distortions caused by the normal thermal expansion and cooling of the joint. The slopes make it difficult to set meaningful constraints because too much area is included. In one example, a Mylar disk was not detected by the algorithm even though its presence is clearly visible in the D-scan. Late in the project GTI realized that the individual A-scans that comprise the D-scan can be shifted to compensate for the shape of the coupling, thereby causing the reflections from the EF wires to be parallel to the x-axis. If this transformation were performed, the evaluation parameters would be greatly improved, and would improve the quality of the results. Figure 44 demonstrates ultrasonics is able to detect aluminum disks as small as 2.4 mm. The 2.0 mm disks were not detected; which is similar to the results obtained by one of the phased array studies (ref 14).

As discussed in the section on scan pattern for the EF saddle tees, the flaws are easily observable. The same algorithm used for the EF couplings would also be used for the EF saddle tees, with corrections for the different thicknesses of the saddle tee base. Adjustment for the varying base thickness would also be made.

There is a large range of pipe diameters and fitting sizes. By making adjustments for the different dimensions, the same algorithms would be used for any pipe size.

Table 1. Predictions and results for yellow 2-inch diameter non-EF couplings

D-scan	No. of Failed	Pass or Fail?	Correct?	Description of joint
1	0	P	Y	Intended to make good joint
2	0	P	Y	Intended to make good joint
3	0	P	Y	Intended to make good joint
4	4	F	Y	Excess soak time
5	24	F	Y	¼-inch long short stab made by moving cold ring in ¼ inch
6	16	F	Y	½ -inch long short stab made by moving cold ring in ½ inch
7	4	F	Y	Did not clean pipe or coupling with alcohol; pipe not chamfered
8	17	F	Y	Pipe pressed in properly, then pulled back ¼-inch
9	30	F	Y	Long stab by ¼-inch.
10	4	F	Y	Dwell time of 10 seconds
11	0	P	Y	Poured fine dry dirt over part of pipe while it was hot
12	11	F	Y	Pushed coupling on properly and twisted pipe approximately 50°
13	14	F	Y	0.092-inches holes drill in inner surface of coupling
14	28	F	Y	V-groove cut in coupling
15	14	F	Y	0.059 and 0.092 inch diameter holes
16	2	F	Y	Insufficient couplant. Intended to make good joint
17	0	P	Y	Intended to make good joint
18	2	F	N	Intended to make good joint
19	15	F	N	Intended to make good joint
20	0	P	Y	Intended to make good joint
21	0	P	Y	Intended to make good joint
22	4	F	Y	425 ^{o}F and 30 seconds. Insufficient heating temperature; excess heating time
23	16	F	Y	425 ^{o}F and 23 seconds. Insufficient heating temperature; normal heating time
24	0	P	N	560 ^{o}F and 30 seconds. Excess heating temperature; excess heating time
25	5	F	Y	560 ^{o}F and 23 seconds. Excess heating temperature; regular heating time
26	6	F	Y	Downward push on fitting clamp
27	8	F	Y	Misalignment causing a “drag” of the melt at the position marked top
28	4	F	Y	Intended to make good joint
29	0	P	Y	Intended to make good joint
30	11	F	Y	610 ^{o}F and 19 seconds
31	8	F	Y	615 ^{o}F and 19 seconds
32	4	F	Y	610 ^{o}F and 19 seconds
33	1	F	Y	378 ^{o}F and 19 seconds
34	1	F	Y	Insufficient couplant. 375 ^{o}F and 19 seconds

Table 2. Predictions and results for orange 2-inch diameter non-EF tees

D-scan	No. of Failed	Pass or Fail?	Correct?	Description of joint
1	7	F	Y	Tee #1: Near crack in pipe
2	15	F	Y	Tee #1: Over crack in pipe at identified leak in pipe
3	22	F	Y	Tee #1: Along bottom of tee with angled pipe
4	6	F	Y	Tee #1: Alongside of tee with angled pipe
5	8	F	Y	Tee #1: Alongside of tee with angled pipe
6	22	F	Y	Tee #2: Along top of tee with angled pipe
7	49	F	Y	Tee #2: Along bottom of tee opposite cracked body
8	24	F	Y	Tee #2: Over crack in first leg of tee
9	31	F	Y	Tee #2: Middle leg of tee

Table 3. Predictions and results for yellow 4-inch diameter non-EF saddle tee fittings

D-scan	No. of Failed	Pass or Fail?	Correct?	Description of joint
1	0	P	Y	Intended to make good joint
2	0	P	Y	Attempted to make good joint
3	6	F	Y	Normal preparation, added dry dirt
4	5	F	Y	Series of holes 1/16 to 1/8 diameter
5	8	F	Y	Normal preparation, added Mobilith AW2 grease
6	8	F	Y	Normal preparation, moved iron back and forth
7	11	F	Y	High temperature fusion 608 ^{o}F
8	5	F	Y	Low temperature fusion 373 ^{o}F

Table 4. Predictions and results for yellow 4-inch diameter EF couplings

D-scan	No. of Failed	Pass or Fail?	Correct?	Description of joint
1	0	P	Y	Intended to make good joint
2	0	P	Y	Intended to make good joint
3	0	P	Y	Intended to make good joint
4	0	P	Y	Intended to make good joint
5	0	P	Y	Intended to make good joint
6	0	P	Y	Pipe was cleaned with alcohol wipe but not scraped
7	0	P	N	Pipe was cleaned with alcohol wipe but not scraped
8	0	P	N	Intended to make good joint
9	5	F	Y	Area contaminated with dry dirt
10	22	F	Y	Area contaminated with mud
11	0	P	N	Area contaminated with a smudge from an oily glove
12	1	F	Y	Area contaminated with dry dirt cutting oil
13	1	F	Y	490 ^{o}F and 175 seconds. Fusion time shortened by 25 seconds
14	0	P	N	490 ^{o}F and 175 seconds. Fusion time shortened by 25 seconds
15	1	F	N	MDPE pipe and HDPE coupling
16	0	P	Y	MDPE pipe and HDPE coupling
17	0	P	??	Curved pipe used to make joint
18	0	P	??	Curved pipe used to make joint
19	0	P	??	Curved pipe used to make joint
20	0	P	??	Curved pipe used to make joint
21	0	P	N	Properly prepared, but joint was moved during cooling
22	0	P	N	Properly prepared, but joint was moved during cooling
23	7	F	Y	6.6 and 12.1 mm disks made from aluminum tape
24	13	F	Y	2.0, 2.4, and 4.7 mm disks made from aluminum tape
25	34	F	Y	38 by 22 mm rectangle made from aluminum tape
26	4	F	Y	2.2, 2.8, and 3.2 mm disks made from aluminum tape
27	0	P	N	2.0 and 4.6 mm disks made from aluminum tape
28	17	F	Y	8.4 and 18.4 mm disks made from aluminum tape
29	0	P	N	6.5, 8.5, and 12.5 mm disks made from Mylar
30	0	P	N	3.1 and 4.6 mm disks made from Mylar
31	0	P	N	Two thin strips made from aluminum tape
32	0	P	N	V-groove cut into pipe
33	0	P	N	2.9 mm diameter holes drilled into pipe at various depths
34	0	P	N	4.9 mm diameter holes drilled into pipe at various depths

Conclusions

- The co-funding portion of the project demonstrated a method of automatically classifying butt fusion joints. The ultrasonic technique requires a modest number of independent parameters and dependent parameters determined from measurements of good joints. The technique does not require the operator to view the waveforms, let alone analyze them.

- This approach was successfully extended to detection of flaws in the other heat fusion jointing methods used for polyethylene pipe. The project developed algorithms that successfully classify heat fusion joints. A practical system will require development of scanning hardware and firmware, followed by more rigorous testing and refinement of the classification algorithms.

- Detection of ovality and angle of pipe insertion of the pipe can be determined after completion of the fusion process.

- Build-up of displaced plastic material inside of non-EF socket couplings and tees can be detected ultrasonically.

- The large number of saddle tee base geometries and obstruction of data collection by the body of the tees limits the amount of the fusion interface that can be ultrasonically inspected.

Recommendations

- Perform research to determine the maximum acceptable angle of insertion of a pipe into the heat fusion coupling or tee. Develop a standard analogous to that of ovality limits.

- Perform research to determine the relationship of material at the end of non-EF couplings and tees and the development of stress risers that would lead to failure with time of otherwise properly made joints.

- Develop hardware and software to automate the inspection process. Use this equipment to expand the testing program and farther refine the discrimination algorithms.

List of Acronyms

HDPE	high density polyethylene
IPS	iron pipe size
MDPE	medium density polyethylene
NDE	non destructive evaluation
NFP	non for profit
PE	polyethylene
SDR	standard dimension ratio (the ratio of pipe diameter to wall thickness)

References

1. Dziengielewski, E., "Ultrasonic Examination of Heatfused Polyethylene Pipe Joints," presented at the AGA Distribution Conference 1973, 73-D-23 pages 226-229.
2. ASTM F 600 – 78 Standard Practice for Nondestructive Ultrasonic Evaluation of Socket and Butt Joints of Thermoplastic Piping.
3. House, L., Lustiger, A., Hyatt, R., Cassady, M., and Smith, R., "Quality Assurance of Heat Fused Polyethylene Plastic Pipe Joints" GRI 81/0199 Annual Report, September 1983.
4. House, L. J. and Lustiger, "Automated Ultrasonic Inspection of Polyethylene Butt Fusion Joints" Proceedings Eighth Plastic Fuel Gas Pipe Symposium November 29-30 & December 1, 1983
5. McClinton, M., "GRI Research on Detection of Flaws in Polyethylene Butt Fusion Joints—An Update" AGA Distribution Conference 1985**,** 85-DT-105 pages 311-318.
6. House, L., Lustiger, A., Hyatt, R., Cassady, M., and Smith, R., "Quality Assurance of Heat-Fused Polyethylene Plastic Pipe Joints, Phase III" GRI 85/0284 Final Report, June 1986.
7. McClinton, M., "How to detect flaws in PE pipe butt fusion joints" Pipe Line Industry November 1986 V65 (5): 137, 139, 141.
8. "Inspection Device for Heat-Fused Butt Joints89 pages 453-455. check
9. Light, G. M., Hendrix, G. J., "Ultrasonic Coupling for Gas Pipe Inspection" AGA Distribution Conference 1992 92-DT-76 pages 446-454.
10. Striplin, T. H., "Development of Automatic Ultrasonic Butt Fusion Joint Inspection for Additional Polyethylene Pipe Diameters" Final Proprietary Report for GRI contract 5091-271-2341 Sept 1996.
11. Striplin, T. H., "Ultra-Mc® –An Ultrasonic system for Evaluating Butt Fusion Joints in PE Pipe" GRI-96/0192.
12. Shin, H. J., Jang, Y. H., Kwan, J. R., and Lee, E. J. "Nondestructive Testing of Fusion Joints of Polyethylene Piping by Real Time Ultrasonic Imaging," NDT.net Mar 2005 Vol. 10 No.3.
13. Bird, C., Caravaca, D., Kleiner, D., "Ultrasonic Phased Array Inspection of Electrofusion Joints in Polyethylene Pipes" ECNDT 2006, Mo.2.6.2
14. Lozev, M., Spencer, R., White, P., Todorov, E., and St. John, M., "Ultrasonic Phased-Array Inspection of Polyethylene Pipe Joints," DOT DTPH56-06-T-0002 and NYSEARCH 49265CSP.
15. Crawford, S. L., Cumblidge, S. E., Doctor, S. R., Hall, T. E., and Anderson, M. T., "NDE," GRI Technology Profile September 1987
16. Rorie, F., "Automated Ultrasonic Butt Fusion Inspection" AGA Distribution Conference 1989, 89-D.
17. Methods on Inspection of HDPE Butt Fusion Joints for Lack of Fusion," Technical Letter Report to U.S. Nuclear Regulatory Commission U.S. DOE contract DE-AC05-76RL01830, May 2008.
18. Kothari, K., Huebler, J.E., Givens, M., and Ziolkowski, "Ultrasonic Inspection of Fusion Welds on PE Mains," OTD 20582 Final Report January 2009.

End of Report